

NASA Contractor Report 4638

# Stability of Separating Subsonic Boundary Layers

---

*Jamal A. Masad*  
*High Technology Corporation • Hampton, Virginia*

*Ali H. Nayfeh*  
*Virginia Polytechnic Institute and State University • Blacksburg, Virginia*

National Aeronautics and Space Administration  
Langley Research Center • Hampton, Virginia 23681-0001

Prepared for Langley Research Center  
under Contracts NAS1-19299 and NAS1-19610

---

December 1994

This publication is available from the following sources:

NASA Center for AeroSpace Information  
800 Elkridge Landing Road  
Linthicum Heights, MD 21090-2934  
(301) 621-0390

National Technical Information Service (NTIS)  
5285 Port Royal Road  
Springfield, VA 22161-2171  
(703) 487-4650

# **STABILITY OF SEPARATING SUBSONIC BOUNDARY LAYERS**

Jamal A. Masad  
High Technology Corporation  
Hampton, VA 23666

and

Ali H. Nayfeh  
Department of Engineering Science and Mechanics  
Virginia Polytechnic Institute and State University  
Blacksburg, VA 24061-0219

## **ABSTRACT**

The primary and subharmonic instabilities of separating compressible subsonic two-dimensional boundary layers in the presence of a two-dimensional roughness element on a flat plate are investigated. The roughness elements considered are humps and forward- and backward-facing steps. The use of cooling and suction to control these instabilities is studied. The similarities and differences between the instability characteristics of separating boundary layers and those of the boundary layer over a flat plate with a zero pressure gradient are pointed out and discussed. The theoretical results agree qualitatively and quantitatively with the experimental data of Dovgal and Kozlov. Cooling and suction decrease the growth rates of primary and subharmonic waves in the attached-flow regions but increase them in the separated-flow regions.

## 1. INTRODUCTION

In boundary-layer flows over aerodynamic surfaces, separation takes place when the adverse pressure gradient exceeds a certain limit. When the flow moves against a pressure gradient, its energy and momentum become too small to overcome the viscous force; as the pressure gradient exceeds a certain value, the flow is brought to rest, and the forward flow then separates from the wall. Separation might occur while the flow is still laminar, so we need to evaluate the influence of separation on the instability waves that can eventually lead to the breakdown of the laminar boundary layer.

In this work, we investigate the stability characteristics of a boundary layer that separates due to the presence of a single, localized two-dimensional roughness element on an otherwise flat plate. The roughness elements considered in this study are humps and forward- and backward-facing steps. Roughness elements exist with varying shapes and dimensions on different aerodynamic surfaces; the importance of determining the shapes and sizes that will allow the flow to remain laminar is evident.

The transition process in a two-dimensional low-speed flow over a two-dimensional roughness element includes such mechanisms as the enhancement of receptivity of free-stream turbulence and acoustic disturbances;<sup>1-4</sup> linear amplification of Tollmien-Schlichting (TS) waves and shear-layer instability for separated flows;<sup>5-8</sup> Görtler instability; enhancement of secondary instabilities;<sup>9-11</sup> and nonlinear interactions that can be captured by nonlinear parabolized stability equations (nonlinear PSE) or direct numerical simulation (DNS) studies of the full Navier-Stokes (NS) equations.<sup>12-14</sup> Localized surface roughness contributes to the generation of disturbances in boundary layers (boundary-layer receptivity) by providing appropriate conditions for the interaction of free-stream acoustic or vortical disturbances with the unsteady motion of the boundary layer. As a result, the disturbances become internalized into the boundary layer. Nayfeh and Ashour<sup>3</sup> found that the receptivity of incompressible boundary-layer flow over a hump to free-stream acoustic waves increases as the hump height increases. When the hump height was sufficient to cause separation, the receptivity increased considerably. The TS and shear-layer instability waves in a separation bubble were found to coexist in flow over a roughness element. Although the shear-layer instability waves are associated with high frequencies, the TS waves are difficult to distinguish from the shear-layer instability waves. The Görtler vortices in the flow over a roughness element develop in the concave surface regions and may interact with the TS waves. Although such interactions are weak<sup>15,16</sup> in flow over a smooth surface, this same result may not occur in the presence of a roughness element. The subharmonic secondary instability increases<sup>9,10</sup> dramatically in a flow that separates due to a roughness element. Such an instability can set a three-dimensionality in the flow field and can lead to early transition. The fundamental secondary instability and nonlinear

interactions may play a significant role in the breakdown to transition when the amplitudes of the disturbances are large enough to cause such interactions.

A major difficulty in studying the stability characteristics of separating flows is the determination of the mean flow. Although conventional boundary layers predict the location of separation, they fail to march through it. Moreover, conventional boundary layers fail to accurately predict the mean flow over roughness elements that do not even cause separation due to the abrupt change in the boundary conditions, which causes viscous-inviscid coupling and adds an upstream influence. Thus, the mean-flow problem must be solved with a triple-deck formulation, an interacting boundary-layer (IBL) method, or a NS solver. For smooth roughness elements with separating and reattaching boundary layers (i.e., small separation bubbles), IBL can be used to accurately determine the flow field. If the roughness elements are sharp or if the size of the element is large enough to induce massive separation and vortex shedding, then both the triple-deck and IBL formulations break down, and a NS solver must be used. Note that to accurately predict the flow field in the presence of roughness elements that may induce separation with a NS solver, one must use a grid that is fine enough to avoid a smearing of the important flow structures by the truncation error or the artificial dissipation. Even for the simple case of a subsonic flow over a smooth flat plate with zero pressure gradient, caution must be exercised in using a NS solver to generate mean-flow profiles if a stability analysis is to be performed on these profiles.<sup>17</sup> Furthermore, because the number of flow cases that must be investigated in linear stability studies is very large, the NS calculations may be very expensive. Lessen and Gangwani<sup>18</sup> and Singh and Lumley<sup>19</sup> used approximate analytical-numerical methods to calculate the velocity profiles in a flow over a roughness element. They found that the calculated profile has an inflection point. By performing temporal linear stability calculations on their calculated velocity profiles, Lessen and Gangwani<sup>18</sup> showed that the roughness has a destabilizing effect and shifts the branch I neutral point toward lower Reynolds numbers, particularly at relatively large streamwise wave numbers.

For the results presented in this work, an IBL formulation was used to calculate the mean flow. The mean-flow profiles generated by IBL and their stability characteristics compared well<sup>20</sup> with those generated with a NS solver and a sufficiently fine grid. However, the IBL formulation is less computationally demanding than NS solvers.

More experimental studies exist than analytical and numerical studies that deal with the stability of separating boundary layers. However, most of these experiments are concerned with determining the transition location (natural transition experiments) and its variation with the relevant parameter space, rather than with the determination of the spectral structure and the growth and development of the instability waves (controlled or forced experiments). Many of these natural transition experiments are, in fact, flight experiments performed on swept and unswept wings. These experiments examine a variety of effects including suction, pressure gradients, compressibil-

ity, and multiple, three-dimensional, and sharp roughness elements. This variation makes the validation of stability theories for separating flows difficult, particularly because DNS studies of the full NS equations of separating flows are rare. These experiments have resulted in several empirically based criteria<sup>21,22</sup> for the prediction of the transition location in flows over roughness elements. However, these criteria are not broadly applicable and are valid only for the considered configurations and experimental conditions. Moreover, these criteria do not provide an understanding of the physical mechanisms that are involved.

In this work, we investigate the stability characteristics of the flow over three types of roughness elements: humps and backward- and forward-facing steps. We focus our attention on roughness elements that induce small separation bubbles. The similarities and differences between the stability characteristics of separating boundary layers and boundary layers on smooth flat plates with a zero pressure gradient are demonstrated and discussed. In Section II we outline the mathematical formulation and the methods of solution; in Section III we present stability results for separating boundary layers; in Section IV we compare our stability results with the experimental data of Dovgal and Kozlov;<sup>23</sup> in Section V we consider the laminar flow control (LFC) of separating boundary layers by cooling and suction; and, finally, in Section VI we present our conclusions.

## 2. FORMULATION AND METHODS OF SOLUTION

### 2.1. Mean Flow

We consider a two-dimensional compressible subsonic steady flow over a smooth two-dimensional localized roughness element on a flat plate. The roughness elements considered in this work include smooth humps and backward- and forward-facing steps. The shape of the hump is given by

$$y = \frac{y^*}{L^*} = \left( \frac{h^*}{L^*} \right) f(z) = hf(z) \quad (1)$$

where

$$f(z) = \begin{cases} 1 - 3z^2 + 2|z|^3, & \text{if } |z| \leq 1 \\ 0, & \text{if } |z| > 1 \end{cases} \quad (2)$$

$$z = 2 \frac{x^* - L^*}{\lambda^*} = 2 \frac{x - 1}{\lambda} \quad (3)$$

Here,  $h^*$  is the hump height,  $\lambda^*$  is the length of the hump,  $L^*$  is the streamwise distance from the leading edge of the flat plate to the center of the hump, and the star denotes a dimensional quantity. The reference length  $L^*$  affects the calculations through the Reynolds number  $Re$ , where

$$Re = \frac{U_\infty^* L^*}{\nu_\infty^*} \quad (4)$$

and  $U_\infty^*$  and  $\nu_\infty^*$  are the free-stream velocity and kinematic viscosity, respectively.

The shape of the step is given by

$$y = (h)g(x), \quad g(x) = \frac{1}{2}\sqrt{Re} \left\{ 1 + \operatorname{erf} \left[ \frac{\pi\sqrt{\pi}s(x-1)}{180h} \right] \right\} \quad (5)$$

where  $h = h^*/L^*$  is the nondimensional height of the step,  $s$  is the slope of the step (negative for a backward-facing step and positive for a forward-facing step), and  $\operatorname{erf}$  is the error function.

Because the roughness elements under consideration may induce separation bubbles, a strong viscous-inviscid interaction and an upstream influence exist. Hence, the conventional boundary-layer formulation fails to predict such flows. In this paper, we use an IBL formulation to solve for the mean flow over the roughness element. For details of the IBL formulation, we refer the reader to Ragab et al.<sup>20</sup>

## 2.2. Primary Instability

To study the stability of the calculated mean profiles, small unsteady two-dimensional disturbances are superimposed on them. Then, we substitute the total flow quantities into the Navier-Stokes equations, subtract the mean flow, invoke the quasiparallel assumption, and linearize the resulting equations with respect to the disturbance quantities. Next, we assume that the disturbance quantities have the so-called normal mode form; that is,

$$\hat{q} = \xi(y) \exp \left[ i \left( \int \alpha dx - \omega t \right) \right] + cc \quad (6)$$

where  $\hat{q}$  stands for a disturbance quantity,  $cc$  denotes the complex conjugate of the preceding term,  $x$  is the streamwise coordinate,  $t$  is time, and  $\alpha$  and  $\omega$  are complex in general. In the stability analyses and computations throughout this work, the reference length is  $\delta_r^* = \sqrt{\nu_\infty^* x^* / U_\infty^*}$ , the reference velocity is  $U_\infty^*$ , the reference time is  $\delta_r^* / U_\infty^*$ , and the pressure is made nondimensional with respect to  $\rho_\infty^* U_\infty^{*2}$ , where  $\rho_\infty^*$  is the free-stream density. For the spatial stability considered in this work,  $\omega$  is real, and  $\alpha = \alpha_r + i\alpha_i$  is complex, where  $\alpha_r$  is the streamwise wave number and  $-\alpha_i$  is the spatial growth rate. The frequency  $\omega$  is related to the dimensional circular frequency  $\omega^*$  through  $\omega = \omega^* \delta_r^* / U_\infty^*$ ; this relationship and the definition of  $\delta_r^*$  show that

$$\omega = FR \quad (7)$$

where

$$F = \frac{\omega^* \nu_\infty^*}{U_\infty^{*2}} \quad (8)$$

and

$$R = \frac{U_\infty^* \delta_r^*}{v_\infty^*} = \sqrt{x Re} \quad (9)$$

Because  $\omega^*$  is fixed for a certain physical wave as it propagates downstream, equation (8) shows that  $F$  is also fixed for the same wave.

Equation (6) can be substituted into the stability equations and boundary conditions to obtain an eigenvalue problem that is solved numerically. The effect of nonparallelism on the two-dimensional instability waves in incompressible flow over a roughness element that might cause separation was studied by Nayfeh and Ashour.<sup>3</sup> The effect was destabilizing but negligible. Spatial DNS studies<sup>12-14</sup> on the effects of nonparallelism on flow stability over a roughness element showed a similar result. Details of the formulation for the linear quasi-parallel primary instability of compressible flows are available in many references (e.g., Mack<sup>24</sup>).

In this paper, we consider subsonic flows with a free-stream Mach number  $M_\infty$  of less than or equal to 0.8. For these flows, at most one unstable primary mode exists for certain flow and stability parameters, and the most unstable primary wave is two dimensional.<sup>24</sup> In all compressible results presented here, the free-stream temperature is 300 K, the Prandtl number is 0.72, and the variation of viscosity with temperature is governed by the Sutherland formula.

### 2.3 Secondary Instability

In the several stages of transition from a laminar to a turbulent boundary layer over a flat plate, the primary instability of two-dimensional TS waves is followed by the appearance of a spanwise variation in the disturbance field. This variation increases and eventually sets in strong three-dimensionality in both the disturbance field and the mean flow.

We now believe that the spanwise variation and, consequently, the three-dimensionality are due to a parametric excitation of low-amplitude three-dimensional disturbances by large-amplitude two-dimensional TS waves. Depending on the relation between the frequencies and the streamwise wave numbers of the exciting (primary) and excited (secondary) waves, we can distinguish between two types of resonances that lead to two types of breakdown to transition.<sup>25,26</sup> When the frequency and streamwise wave number of the three-dimensional wave are equal to one-half those for the two-dimensional wave, we have a subharmonic resonance that leads to the H-type of breakdown. On the other hand, when the frequencies and streamwise wave numbers of the primary and secondary waves are equal, we have a fundamental parametric resonance that leads to the K-type of breakdown.

The secondary instability of incompressible boundary-layer flows over a smooth flat plate was studied extensively by Herbert,<sup>25,26</sup> and later extended to compressible flow by Nayfeh,<sup>27</sup> El-Hady,<sup>28</sup> Masad and Nayfeh,<sup>29</sup> and Ng and Erlebacher;<sup>30</sup> details of the formulation are available in these references.



## 2.4 Validation of Mean-Flow and Stability Codes

For smooth surfaces, one can use a conventional boundary-layer formulation to solve for the mean flows over these surfaces. However, conventional boundary-layer formulations cannot accurately predict the flow over surfaces with abrupt changes in the boundary conditions because of the strong viscous-inviscid interaction and the possibility of flow separation. Instead, one needs to use a triple-deck formulation, an IBL formulation, or a NS solver. These approaches account for the viscous-inviscid interaction, as well as separation bubbles, but NS solvers are very expensive in comparison with triple-deck and IBL formulations.

To validate the IBL approach, Ragab et al.<sup>20</sup> compared their results for a backward-facing step with solutions to the thin-layer compressible NS equations. They used the computer code ARC2D. The mean flows as well as the stability characteristics were compared. They found that for the purpose of stability analysis of boundary layers over smooth-surface roughness elements, the IBL formulation is a viable alternative to the NS equations.

The stability results presented in this paper were calculated with finite differences.<sup>31</sup> The primary instability code was validated by comparing its results for incompressible and compressible flows with the results produced by the fundamental matrix method.<sup>32</sup> Ng and Erlebacher<sup>30</sup> found that our results<sup>29</sup> (from the subharmonic instability code) agree well with their results.

## 3. STABILITY RESULTS

Nayfeh et al.<sup>5</sup> studied theoretically the primary instability of incompressible flows over two-dimensional humps and dips. They found that the instability depends on the height-to-width ratio of the roughness element as well as the location of the element with respect to branch I of the Blasius neutral stability curve. Moreover, they pointed out that the stability of separating flows is more complicated than the stability of flows over smooth surfaces due to the coexistence of viscous and shear-layer instability mechanisms. The major findings of Nayfeh et al.<sup>5</sup> were also reached by Cebeci and Egan.<sup>6</sup>

To gain insight into the physics of the instability of flows over roughness elements, Nayfeh et al.<sup>5</sup> analyzed the streamwise distribution of the pressure coefficient  $C_p$ . A typical streamwise distribution of the pressure coefficient for a separating flow over a hump is shown in Figure 1. Note that for all humps considered in this work, the center is located at  $x = 1.0$ , which means that for  $Re = 10^6$  the value of  $R$  at the center is  $R = \sqrt{xRe} = 1000$ . The symmetric hump extends between  $x = 0.9$  and  $1.1$ . With the center located at  $R = 1000$ , separation starts downstream of the center of the hump. An adverse-pressure-gradient region is located ahead of the hump and is followed by a region of favorable pressure gradient that extends over a very short distance. Then a strong adverse pressure gradient occurs, which causes the boundary layer to separate; then another region of favorable pressure gradient begins. Thus, we expect that the primary instability waves will be unstable ahead of

the hump (Figure 2), become stable over the short favorable-pressure-gradient region, become unstable again in the separation region, and finally, become stable in the second favorable-pressure gradient region.

Next, we consider a boundary layer that separates due to the presence of a backward-facing step. Except for comparison with the experimental data in Section IV, all steps considered in this work are centered at  $x = 1.0$ , and for  $Re = 10^6$  they are centered at  $R = 1000$ . In Figure 3, we show the streamwise distribution of the pressure coefficient. The vertical dashed lines are the streamwise boundaries of the separation bubble. Far upstream and far downstream of the step, the pressure coefficient approaches that of the flow over a smooth flat plate; hence we expect that the stability characteristics in these regions approach those of the flow over a smooth flat plate. In contrast with the case of the hump (where we have four regions of pressure gradient), in the case of the flow over the backward-facing step, we have only three regions: a short favorable-pressure-gradient region, followed by a strong adverse-pressure-gradient region that could cause the flow to separate, and another region of favorable pressure gradient. Consequently, the step will have a stabilizing influence in the favorable-pressure-gradient regions and a destabilizing influence in the adverse-pressure-gradient region.

In Figure 4, we compare the neutral stability curve for the flow over a flat plate without a roughness element with that for the flow in the presence of a backward-facing step. Far away from the step, the neutral curve approaches that of the Blasius flow, as expected. The first region of favorable pressure gradient divides the unstable region into two regions. The second favorable-pressure-gradient region reduces the instability. Moreover, the strong adverse pressure gradient, which is responsible for separation, causes part of the right unstable region to extend over a very large band of frequencies. The unstable high-frequency disturbances in the flow over the step are a strong indication of the inviscid nature of the instability in the separation region. This instability is similar to mixing and shear-layer instabilities. The inviscid and high-frequency instabilities in the flow over a square hump were found in the DNS study of Danabasoglu et al.<sup>14</sup> Furthermore, Klebanoff and Tidstrom<sup>8</sup> found that close to the roughness element the fluctuation was composed of relatively higher frequencies. In our search for branch I of the neutral stability curve in the adverse-pressure-gradient region of figure 4, we encountered an interval of  $R$  in which the stability code converged on negative frequencies, which means that in this interval the flow is unstable regardless of how small is the frequency. The wave numbers (Figure 4(b)) associated with these unstable low-frequency disturbances are very small. One of the consequences of the presence of a stable region that divides the unstable region into two regions is that if we follow a wave with a fixed frequency as it is convected downstream, then as we march through the stable region, it is easy to converge at and keep following one of the several damped modes that exist, especially if the initial guess of the eigenvalue is extrapolated from previous streamwise solutions. We encountered this situation in

comparing our theoretical results with the experimental data of Dovgal and Kozlov<sup>23</sup> for the case of a forward-facing step with a relatively large height. In this type of situation, a global numerical eigenvalue scheme has a distinct advantage over a local one.

The movement of the transition location as the height of the roughness element varies is an important consideration (Schlichting<sup>33</sup>). Earlier papers on this problem assumed that the point of transition is located at the position of the roughness element when the roughness element is relatively large or that the presence of the roughness element has no influence when it is relatively small. However, Fage<sup>21</sup> (Schlichting<sup>33</sup>) has shown experimentally that the point of transition moves continuously upstream as the height of the roughness element is increased, until it ultimately reaches the position of the roughness element. Schlichting<sup>33</sup> pointed out that in discussing the influence of roughness on transition, three questions must be answered. First, what is the maximum height of a roughness element below which the element has no influence on transition? Second, what is the height of the roughness element that induces transition at the element? Third, how can the transition location be described in the range between these two limits? The answer to the first question has practical applications; if such a critical height exists, then allowable tolerances on unavoidable roughness elements will be designed such that these critical heights are not exceeded. To answer these questions with linear stability theory, we adopt the empirical  $e^N$  ( $N = 9$ ) transition criterion. Thus, we correlate the transition location with the shortest distance, measured from the leading edge, at which the amplification factor ( $N$  factor) of the primary disturbance reaches the value 9. The value of  $R$  at this location is denoted by  $R_{N=9}$ . Thus, we calculate the values of  $R_{N=9}$  and the corresponding values of  $F$  for several hump heights (from  $h = 0$  (no hump) to the nondimensional hump height  $h = 0.004$ ). The variation of  $R_{N=9}$  with the hump height is shown in Figure 5(a); the variation of the corresponding most amplified frequency  $F$  with the hump height is shown in Figure 5(b). In Figure 5, we denote each point at which the calculations were actually made by a circle and join the circles.

Figure 5(a) clearly shows that the theoretically predicted transition location moves continuously upstream as the hump height increases; this result is consistent with the experimental findings of Tani and Hama.<sup>34</sup> (See also Dryden.<sup>35</sup>) However, this variation is not linear. The curve that describes the movement of the location of  $R_{N=9}$  becomes steeper as the hump height increases and becomes steepest when the flow separates. When the hump height exceeds a critical value, the location where  $N$  first reaches 9 moves slowly upstream toward a location only a short distance downstream of the center of the hump, which is the point of onset of separation. The existence of a roughness height at which transition takes place at the roughness element has been noted by many experimentalists (e.g., Dryden<sup>35</sup> and Fage and Preston<sup>36</sup>). This height was correlated based on experimental data by defining a Reynolds number  $Re_h$  such that

$$Re_k = \frac{k^* U_k^*}{\nu^*}$$

where  $k^*$  is the height of the roughness element,  $U_k^*$  is the velocity of the flow at the height  $k^*$  in the absence of roughness, and  $\nu^*$  is the kinematic viscosity. Transition is assumed to occur at the roughness element when  $Re_k$  exceeds a critical value. Fage and Preston<sup>36</sup> estimated this value at 400 for flow past a wire mounted on a body of revolution. However, if the roughness is not a circular wire, then this  $Re_k$  criterion does not take into account the effects of roughness-element length, which was found by Masad and Iyer<sup>7</sup> to be significant. Note in Figure 5(b) that the most amplified frequency increases as the predicted transition Reynolds number decreases and shifts toward a much higher value as the flow separates.

Dryden<sup>35</sup> analyzed previously published data on the effect of both single and distributed roughness on transition from laminar to turbulent flow. Dryden<sup>35</sup> collected the experimental data points of Tani and Hama,<sup>34</sup> Tani et al.,<sup>37</sup> Stüper,<sup>38</sup> and Scherbarth (as reported in Quick<sup>39</sup>) and showed that the ratio  $Re_t / Re_0$  of the transition Reynolds number  $Re_t$  on a rough plate to the transition Reynolds number  $Re_0$  on a smooth plate correlates reasonably well with the ratio  $k / \delta_k^*$  of the roughness height  $k$  to the displacement thickness  $\delta_k^*$  of the boundary layer at the location of the roughness element. The resulting correlation is similar to that in figure 5(a), although the region in figure 5(a) at which transition takes place at the roughness element is missing in Dryden's figure. However, Dryden indicated in his comments on the correlation results that the "curve applies only when transition occurs downstream from the roughness element." Dryden<sup>35</sup> also investigated the existence of a roughness height at which transition takes place at the roughness element. In analyzing the experimental data of Tani and Hama,<sup>34</sup> he indicated that "departures from a single functional relation between  $Re_t$  and  $k / \delta_k^*$  occurred as the transition position approached the position of the roughness element." The existence of two functional relations between  $Re_t$  and  $k$  is clear in figure 5(a).

In Figures 6(a) and 6(b), we show the streamwise variations of the growth rates and  $N$  factors for three points shown in Figure 5. The hump height that causes incipient separation for the conditions in Figure 5 is  $h = 0.0021$ . In dimensional quantities, the hump height is

$$h^* = \frac{h Re \nu_\infty^*}{U_\infty^*} \quad (8)$$

So, for  $Re = 10^6$ ,  $h = 0.0021$ , and a unit Reynolds number of  $10^6/\text{ft}$ , the hump height that causes incipient separation is 0.0252 in or 0.65 mm; this value increases as the unit Reynolds number decreases.

Nayfeh et al.<sup>9</sup> studied the effect of a bulge on the subharmonic instability of incompressible boundary layers. They examined the effect of the hump height on the growth rate and amplification

factor of the subharmonic wave for five disturbance frequencies. They found that in the absence of separation an increase in the hump height results in an increase in the amplification factors of the primary and subharmonic waves at all considered frequencies. The amplification factors when separation occurs are much larger than those when no separation occurs. In the subharmonic instability results in this paper, the amplitude of the primary wave is defined as the root mean square (rms) of the streamwise velocity disturbance maximized over the normal coordinate. The spanwise wave-number parameter  $B = 1000 \beta/R$  (where  $\beta$  is the spanwise wave number of the subharmonic wave) of the most amplified subharmonic wave shifts<sup>9,10</sup> toward smaller values of  $B$  as the hump height increases.

#### 4. COMPARISON WITH EXPERIMENTAL DATA

Nayfeh et al.<sup>5</sup> studied the primary instability characteristics of incompressible flows over two-dimensional humps and dips mounted on a flat plate. They compared their theoretical results with the natural transition experimental data of Walker and Greening as reported in Fage.<sup>21</sup> In these experiments, the maximum transverse dimension of the roughness element varied from 0.75 mm (0.03 in.) to 1.75 mm (0.07 in.) for the humps and from 1.425 mm (0.057 in.) to 1.675 mm (0.067 in.) for the dips. The free-stream mean-flow velocities ranged from 15.9 m/sec (53.0 ft/sec) to 28.5 m/sec (95.0 ft/sec) for the humps, and from 18.57 m/sec (61.9 ft/sec) to 25.47 m/sec (84.9 ft/sec) for the dips. Nayfeh et al.<sup>5</sup> followed a primary wave with a fixed physical frequency from the onset of instability (branch I) to the experimentally determined transition location, computed the value of the  $N$  factor at that location, changed the frequency, repeated the calculations, and so on. The frequency that resulted in the maximum value of the  $N$  factor at the experimentally determined transition location was taken as the frequency of the disturbance wave that causes transition. Nayfeh et al.<sup>5</sup> compared their theoretical results with 14 sets of experimental results for humps and 6 sets of experimental results for dips. The calculated mean flows show that 13 out of the 14 humps induce separation, and all 6 dips induce separation. The theoretically calculated values of the  $N$  factors at the experimentally determined transition locations in the hump cases vary from  $N = 7.4$  to 10.0, with an average value of 8.5. For the cases with dips, these values vary from  $N = 6.7$  to 9.2 with an average value of 8.0. This comparison increases the confidence in using the empirical  $e^N$  method as a tool for predicting the transition location.

Fage<sup>21</sup> used his own experimental data on the effects of surface roughness on transition, as well as the experimental data of Walker and Greening, Walker and Cox, and Hislop (as reported in Fage<sup>21</sup>), to correlate the transition location with the height  $h$  and length  $\lambda$  of the roughness element and the Reynolds number  $Re$ . Masad and Iyer<sup>7</sup> took various combinations of  $h$ ,  $\lambda$ , and  $Re$  for flows over a hump and computed the predicted transition location with linear stability theory and the  $e^9$

method and compared their results with the results of the correlation of Fage.<sup>21</sup> The agreement between both sets of results is good.

Dovgal and Kozlov<sup>23</sup> conducted a controlled (forced) experiment to study the influence of imperfections on the stability characteristics of incompressible flows. They used a vibrating ribbon placed upstream of a roughness element to introduce two-dimensional small-amplitude disturbances into the developing boundary layers. Dovgal and Kozlov considered a hump, a forward-facing step, and a backward-facing step. In the hump cases, the experimentally determined distributions of the magnitudes of the streamwise velocity fluctuations across the boundary layer exhibit the same three-peak characteristics predicted theoretically by Nayfeh et al.<sup>5</sup> As demonstrated by Nayfeh et al.,<sup>5</sup> the distribution of the magnitude of the streamwise velocity fluctuation of a flow over a smooth surface across the boundary layer has two peaks, a large one at the critical layer and a small peak near the edge of the boundary layer. In the separation region, the distribution develops a third peak at the inflection point of the mean-flow profile. This peak is due to the shear-layer instability mechanism, and it increases in magnitude with distance from the separation point, achieves a maximum that can be comparable to the peak at the critical layer, and then decreases to zero at the reattachment point. The experimentally determined transverse and streamwise developments of the disturbances ahead, inside, and after the separation bubble are similar to those obtained by Nayfeh et al.<sup>5</sup> Moreover, our calculated distribution of the phase of the streamwise velocity disturbance across the separating boundary layer has the same two-phase jump as that measured by Dovgal and Kozlov.<sup>23</sup> The three peaks in the transverse distribution of the streamwise velocity fluctuation and the corresponding two-phase jump were also found<sup>40</sup> in subsonic flow on a smooth surface that exhibits an adverse pressure gradient because of its curvature. The same three-peak characteristic in the transverse distribution of the streamwise velocity fluctuation was found in the DNS results of Danabasoglu et al.<sup>14</sup> for the flow over a square hump, which agrees with the experimental data of Boiko et al.<sup>41</sup>

In the step cases, the center of the step was located 500 mm downstream of the leading edge of the plate, the free-stream velocity was 6 m/s, and the Reynolds number based on the distance from the leading edge to the center of the step and the free-stream velocity was  $2 \times 10^5$ . Two step heights were used: 0.9 and 2.2 mm; the vibrating ribbon was excited by three different frequencies: 60, 76, and 94 Hz. In nondimensional quantities, the heights were  $h = 0.9/500 = 0.0018$ , and  $h = 2.2/500 = 0.0044$ . The nondimensional frequencies were  $F = 157 \times 10^{-6}$ ,  $199 \times 10^{-6}$ , and  $246 \times 10^{-6}$ . Dovgal and Kozlov<sup>23</sup> reported the streamwise variation of the integral of the growth rates. The 12 cases presented by Dovgal and Kozlov are compared with our theoretical calculations in Figure 7. The overall agreement is good and supports the calculation of the mean flow with IBL and the calculation of the growth rates with the quasi-parallel linear stability theory.

The IBL results predict that the flow separates when the step height is 2.2 mm, regardless of whether the step is a forward- or backward-facing one. When the height is 0.9 mm, the IBL results

predict no separation for both types of steps. We point out here that the work of Dovgal and Kozlov<sup>23</sup> does not clearly state how sharp the steps used in the experiments were. Their sketch of the steps suggests that they were very sharp; if this assumption is true, then some of the theoretical underpredictions in the experimental results might be attributed to the fact that the calculations were performed with smooth steps.

## 5. LAMINAR FLOW CONTROL OF SEPARATED BOUNDARY LAYERS

Laminar flow control (LFC) is the art and science of delaying or enhancing (depending on the application) the occurrence of laminar-turbulent transition. In subsonic boundary-layer flows over commercial aircraft surfaces, increased efficiency can be realized by maintaining larger regions of laminar flow to reduce friction and drag; increased efficiency can translate into larger range, reduced volume, and fuel cost savings. Because aerodynamic surfaces have some degree of roughness either from manufacturing irregularities or environmental conditions, the study of LFC techniques is of practical importance.

These techniques are known to be most effective when applied to low-amplitude fluctuations; that is, when the disturbances are in the linear regime and before the onset of any significant wave interactions. However, in this section, we consider the effect of LFC techniques on both primary and subharmonic disturbances. Although subharmonic disturbances dominate at a somewhat significant amplitudes of the primary wave, the interest here is in studying the response of existing subharmonic waves to the different LFC techniques that are applied to control the initial stages of primary-disturbance growth.

### 5.1 Effect of Compressibility

For flow over a flat plate,<sup>24,28–30</sup> the overall effect of compressibility is stabilizing following a primary or a subharmonic wave as the wave propagates downstream. In Fig. 8, we show the effect of compressibility on the neutral two-dimensional primary instability curves. The neutral curves for  $M_\infty = 0.8$  are lower (smaller frequencies and streamwise wave numbers) than those that correspond to incompressible flow. The maximum growth rates (maximized over all frequencies) for  $M_\infty = 0.8$  and  $M_\infty = 0$  are compared in Fig. 9. Compressibility is clearly stabilizing.

The effect of compressibility on the stability of flows over imperfections is not the same as its effect on flows over a flat plate. An increase in the Mach number increases the streamwise extent of the separation bubble (Fig. 10). In Fig. 10, we show the variation of the streamwise locations of the separation and reattachment with hump height for  $M_\infty = 0$  and 0.8. For a given Mach number  $M_\infty$  and a given hump height  $h$ , the left branch corresponds to the separation location, whereas the right branch corresponds to the reattachment location. As the Mach number increases, the separation location moves slightly upstream, but the reattachment location moves significantly downstream.

The increase in the size of the separation bubble due to compressibility is consistent with the experimental findings of Larson and Keating.<sup>42</sup> The increase in the size of the separation bubble due to compressibility causes a destabilization of the flow that counters the stabilizing effect of compressibility in the attached-flow regions. However, Masad and Iyer<sup>7</sup> showed that the overall effect of compressibility on the predicted transition Reynolds number with the  $e^N$  method is stabilizing. Their findings are consistent with the experimental findings.<sup>43,44</sup>

## 5.2 Effect of Heat Transfer

The effect of heat transfer on the primary instability of compressible boundary layers over a flat plate was studied extensively by Mack.<sup>24</sup> Mack found that cooling stabilizes first-mode waves. Masad and Nayfeh<sup>45</sup> and El-Hady<sup>46</sup> studied the effect of heat transfer on the subharmonic instability of compressible flows over a smooth flat plate. They found that the direct effect of cooling (the amplitude of the primary wave is fixed) on the subharmonic wave in incompressible flows is very small and becomes destabilizing at large amplitudes of the primary wave. They also found that when the primary wave is a first mode, cooling stabilizes the subharmonic wave at low spanwise wave numbers and destabilizes it at high spanwise wave numbers.

Our mean-flow calculations indicate that cooling delays the occurrence of separation until larger hump heights are introduced; when the flow separates, cooling reduces the size of the separation bubble. These results are consistent with the experimental findings of Larson and Keating.<sup>42</sup>

In the results presented in this subsection, we express the level of heat transfer by specifying the ratio of the actual wall temperature to the adiabatic wall temperature  $T_w/T_{ad}$ . For  $T_w/T_{ad} = 1$ , we have an adiabatic condition; values of  $T_w/T_{ad} < 1$  indicate cooling. The effect of cooling on the primary instability of flows over a hump large enough to induce separation is shown in Figs. 11 and 12 for  $M_\infty = 0$  and 0.8, respectively. If we compare these figures, the stabilizing effect of compressibility is evident. Moreover, Figs. 11 and 12 show clearly that cooling has a stabilizing influence in the attached regions and a destabilizing influence in the separation region.

The effect of cooling on the subharmonic instability of subsonic flows ( $M_\infty = 0.8$ ) over a hump is shown in Fig. 13. At the considered spanwise wave number  $B = 0.2$  and the rms amplitude of the primary wave  $A_{\text{rms}} = 0.01$ , cooling has a stabilizing influence on the subharmonic wave in the attached regions and a strong destabilizing influence on this wave in the adverse-pressure-gradient regions.

## 5.3 Effect of Suction

Suction is a well-known technique for the LFC of air boundary layers on aerodynamic surfaces. The effectiveness and feasibility of LFC by suction has been demonstrated in both wind-tunnel and flight experiments. The success of these demonstrations has led to the adoption of boundary-layer



suction as a method for maintaining larger regions of laminar flow on the wings of newly designed aircrafts.

Suction stabilizes primary disturbances in both incompressible and compressible flows over smooth flat plates. Moreover, El-Hady<sup>47</sup> found that suction stabilizes subharmonic disturbances in incompressible boundary layers. Masad and Nayfeh<sup>48</sup> and El-Hady<sup>46</sup> also showed that suction stabilizes subharmonic disturbances in compressible boundary layers.

To determine the influence of suction on flows over roughness elements, we considered the flow over a backward-facing step with uniform suction. Figure 14 shows the variation of the growth rates of disturbances in incompressible flow over the step with  $R$  in the absence and presence of a uniform suction ( $v_w = -1.0 \times 10^{-4}$ ). The step height is  $h = 0.005$ , and the flow separates with and without suction. The suction used in the calculations for Fig. 14 reduces the size of the separation bubble, which agrees with the experimental findings of Hahn and Pfenninger.<sup>49</sup> Moreover, suction has a stabilizing effect in the attached regions but may have a destabilizing effect in parts of the separation bubble. For small step heights that do not induce separation, suction has a stabilizing effect at all locations.

Although suction has both direct (the amplitude of the primary wave being fixed) and indirect (the amplitude of the primary wave changes) stabilizing effects on subharmonic waves in the case of attached flow, it has a destabilizing direct effect in the separation bubble caused by a backward-facing step, as shown in Fig. 15.

## 6. CONCLUSIONS

The stability characteristics of two-dimensional compressible subsonic boundary layers that separate due to the presence of a two-dimensional roughness element on a flat plate are investigated. The roughness elements considered are humps and forward- and backward-facing steps. The mean-flow problem is solved with the interacting boundary-layer (IBL) equations. The growth rates obtained by using both the IBL equations and the quasi-parallel linear stability theory agree with the forced experimental data of Dovgal and Kozlov.<sup>23</sup>

As the height of the roughness element increases gradually from zero, the theoretically predicted transition location with the  $N$  factor criterion moves continuously upstream. However, the shift in the transition location upstream increases sharply as the hump height approaches the value that corresponds to incipient separation. As the height of the roughness element approaches a certain large value (larger than the value that causes separation), the upstream movement of the predicted transition location slows down considerably. Thus, the transition location is close to the separation point.

Suction and cooling stabilize the attached flow and destabilize the flow in the region of the separation bubble. This result is consistent for both primary and subharmonic disturbances.

To date, the most common and practical approach for predicting the transition location in boundary-layer flows over smooth and rough surfaces is linear stability theory coupled with the empirical  $e^N$  method. However, no theoretically based criteria exist for manufacturing and installation tolerances of roughness elements to prevent or delay transition. Additional stability calculations, numerical simulations, and flight and ground facility experiments are needed, as well as data on the combination of all three approaches, to generate such criteria.

## ACKNOWLEDGMENTS

The research of the first author was supported by the Laminar Flow Control Project Team, Fluid Mechanics and Acoustics Division, NASA Langley Research Center, Hampton, VA under contract no. NAS1-19299. The research of the second author was supported by NASA Langley Research Center, under grant no. NAS1-19610, Task 9.

## REFERENCES

- <sup>1</sup> M. Choudhari and C. L. Streett, "A finite Reynolds-number approach for the prediction of boundary-layer receptivity in localized regions," *Phys. Fluids* **A4**, 2495 (1992).
- <sup>2</sup> J. D. Crouch, "Localized receptivity of boundary layers," *Phys. Fluids* **A4**, 1408 (1992).
- <sup>3</sup> A. H. Nayfeh and O. N. Ashour, "Acoustic receptivity of a boundary layer to Tollmien-Schlichting waves resulting from a finite-height hump at finite Reynolds numbers," Submitted for publication, *Phys. Fluids* (1994).
- <sup>4</sup> M. Wiegel and R. W. Wleziem, "Acoustic receptivity of laminar boundary layers over wavy walls," AIAA Paper 93-3280 (1993).
- <sup>5</sup> A. H. Nayfeh, S. A. Ragab, and A. A. Al-Maaitah, "Effect of bulges on the stability of boundary layers," *Phys. Fluids* **31**, 796 (1988).
- <sup>6</sup> T. Cebeci and D. A. Egan, "Prediction of transition due to isolated roughness," *AIAA J.* **27**, 870 (1989).
- <sup>7</sup> J. A. Masad and V. Iyer, "Transition prediction and control in subsonic flow over a hump," *Phys. Fluids* **6**, 313 (1994).
- <sup>8</sup> P. S. Klebanoff and K. D. Tidstrom, "Mechanisms by which a two-dimensional roughness element induces boundary-layer transition," *Phys. Fluids* **15**, 1173 (1972).
- <sup>9</sup> A. H. Nayfeh, S. A. Ragab, and J. A. Masad, "Effect of a bulge on the subharmonic instability of boundary layers," *Phys. Fluids* **A2**, 937 (1990).
- <sup>10</sup> J. A. Masad and A. H. Nayfeh, "Effect of a bulge on the subharmonic instability of subsonic boundary layers," *AIAA J.* **30**, 1731 (1992).
- <sup>11</sup> T. C. Corke, A. Bar-Sever, and A. V. Morkovin, "Experiments on transition enhancement by distributed roughness," *Phys. Fluids* **29**, 3199 (1986).
- <sup>12</sup> H. Bestek, K. Gruber, and H. Fasel, "Numerical investigation of unsteady laminar boundary layer flows over backward-facing steps," The Fourth Asian Congress of Fluid Mechanics, Hong Kong, 19-23 August 1989.

- <sup>13</sup>S. Elli and C. P. van Dam, "The influence of a laminar separation bubble on boundary-layer instability," AIAA Paper No. 91-3294 (1991).
- <sup>14</sup>G. Danabasoglu, S. Biringen, and C. L. Streett, "Spatial simulation of boundary layer instability: effects of surface roughness," AIAA Paper 93-0075 (1993).
- <sup>15</sup>A. H. Nayfeh and A. A. Al-Maaithah, "Influence of streamwise vortices on Tollmien-Schlichting waves," *Phys. Fluids* **31**, 3542 (1988).
- <sup>16</sup>M. R. Malik, "Wave-interactions in three-dimensional boundary layers," AIAA Paper No. 86-1129 (1986).
- <sup>17</sup>J. A. Garriz, V. N. Vatsa, and M. D. Sanetrik, "Issues involved in coupling Navier-Stokes mean-flow and linear stability codes," AIAA Paper No. 94-0304 (1994).
- <sup>18</sup>M. Lessen and S. T. Gangwani, "Effect of small amplitude wall waviness upon the stability of the laminar boundary layer," *Phys. Fluids* **19**, 510 (1976).
- <sup>19</sup>K. Singh and J. L. Lumley, "Effect of roughness on the velocity profile of a laminar boundary layer," *Appl. Sci. Res.* **24**, 168 (1971).
- <sup>20</sup>S. A. Ragab, A. H. Nayfeh, and R. C. Krishna, "Stability of compressible boundary layers over a smooth backward-facing step," AIAA Paper No. 90-1449 (1990).
- <sup>21</sup>A. Fage, "The smallest size of spanwise surface corrugation which affect boundary layer transition on an airfoil," British Aeronautical Research Council, 2120 (1943).
- <sup>22</sup>B. H. Carmichael, "Surface waviness criteria for swept and unswept laminar suction wings," Northrop Aircraft Report No. NOR-59-438 (BLC-123) (1957).
- <sup>23</sup>A. V. Dovgal and V. V. Kozlov, "Hydrodynamic instability and receptivity of small scale separation regions," *Laminar-Turbulent Transition*, edited by D. Arnal and R. Michel (Springer-Verlag, Berlin, 1990).
- <sup>24</sup>L. M. Mack, "Boundary-layer stability theory," Jet Propulsion Laboratory Report No. 900-277, Rev. A (1969).
- <sup>25</sup>Th. Herbert, "Analysis of the subharmonic route to transition in boundary layers," AIAA Paper No. 84-0009 (1984).
- <sup>26</sup>Th. Herbert, "Secondary Instability of boundary layers," *Ann. Review of Fluid Mech.* **20**, 487 (1988).
- <sup>27</sup>A. H. Nayfeh, "Stability of compressible boundary layers," *Transonic Symposium: Theory, Application, and Experiments*, NASA CP-3020, Vol. 1, Part 1 (1988).
- <sup>28</sup>N. M. El-Hady, "Spatial three-dimensional secondary instability of compressible boundary-layer flows," *AIAA J.* **29**, 688 (1991).
- <sup>29</sup>J. A. Masad and A. H. Nayfeh, "Subharmonic instability of compressible boundary layers," *Phys. Fluids* **A2**, 1380 (1990).
- <sup>30</sup>L. L. Ng and G. Erlebacher, "Secondary instabilities in compressible boundary layers," *Phys. Fluids* **A4**, 710 (1992).
- <sup>31</sup>V. Pereyra, "PASVA3: an adaptive finite-difference Fortran program for first-order nonlinear boundary-value problems," *Lecture Notes in Computer Science* **76**, 67 (1976).
- <sup>32</sup>O. R. Asfar, J. A. Masad, and A. H. Nayfeh, "A method for calculating the stability of boundary layers," *Computers & Fluids* **18**, 305 (1990).

- <sup>33</sup>H. Schlichting, *Boundary-Layer Theory* (McGraw-Hill, Seventh Edition, 1979).
- <sup>34</sup>I. Tani and F. R. Hama, "Some experiments on the effect of a single roughness element on boundary-layer transition, Readers' Forum," *J. Aero. Sci.* **20**, 289 (1953).
- <sup>35</sup>H. L. Dryden, "Review of published data on the effect of roughness on transition from laminar to turbulent flow," *J. Aero. Sci.* **7**, 477 (1953).
- <sup>36</sup>A. Fage and J. H. Preston, "On transition from laminar to turbulent flow in the boundary layer," *Proceedings of the Royal Society of London* **178**, 201 (1941).
- <sup>37</sup>I. Tani, R. Hama, and S. Mituisi, "On the permissible roughness in the laminar boundary layer," *Aero. Res. Inst. Tokyo* **199**, Tokyo (1940).
- <sup>38</sup>J. Stüper, "The influence of surface irregularities on transition with various pressure gradients," Division of Aeronautics, Australia, Report A59, Melbourne (1949), (see also *Aerodynamics Tech. Memos.* 77 and 78).
- <sup>39</sup>A. W. Quick, "Einige Bemerkungen über laminar profile und über das verhalten der laminaren grenss chicht unter dem einfluss von störkörpern," *Lilienthal-Gesellschaft für Luftfahrtforschung, Ber.* 141, Nachtragsbericht.
- <sup>40</sup>J. A. Masad and Y. H. Zurigat, "Effect of pressure gradient on first mode of instability in compressible boundary layers," *Phys. Fluids*, Vol. 6, No. 12, (1994).
- <sup>41</sup>A. V. Boiko, A. V. Dovgal, V. V. Kozlov, and V. A. Shcherbakov, "Flow instability in the laminar boundary layer separation zone created by a small roughness element," *Fluid Dynamics* **25**, 12 (1990).
- <sup>42</sup>H. K. Larson and S. J. Keating, "Transition Reynolds numbers of separated flows at supersonic speeds," *NASA Tech. Note TN D-349* (1960).
- <sup>43</sup>D. R. Chapman, D. M. Kuehn, and H. K. Larson, "Investigation of separated flows in supersonic and subsonic streams with emphasis on the effect of transition," *NACA Report No. 1356* (1958).
- <sup>44</sup>D. Coles, "Measurements of turbulent friction on a smooth flat plate in supersonic flows," *J. Aero. Sci.* **21**(7), 433 (1954).
- <sup>45</sup>J. A. Masad and A. H. Nayfeh, "Effect of heat transfer on the subharmonic instability of compressible boundary layers," *Phys. Fluids* **A3**, 2148 (1991).
- <sup>46</sup>N. M. El-Hady, "Secondary instability of high-speed flows and the influence of wall cooling and suction," *Phys. Fluids* **A4**, 727 (1992).
- <sup>47</sup>N. M. El-Hady, "Effect of suction on controlling the secondary instability of boundary layers," *Phys. Fluids* **A3**, 393 (1991).
- <sup>48</sup>J. A. Masad and A. H. Nayfeh, "Effect of suction on the subharmonic instability of compressible boundary layers," *Phys. Fluids* **A3**, 2179 (1991).
- <sup>49</sup>M. Hahn and W. Pfenninger, "Prevention of transition over a backward step by suction," *J. Aircraft* **10**, 618 (1973).

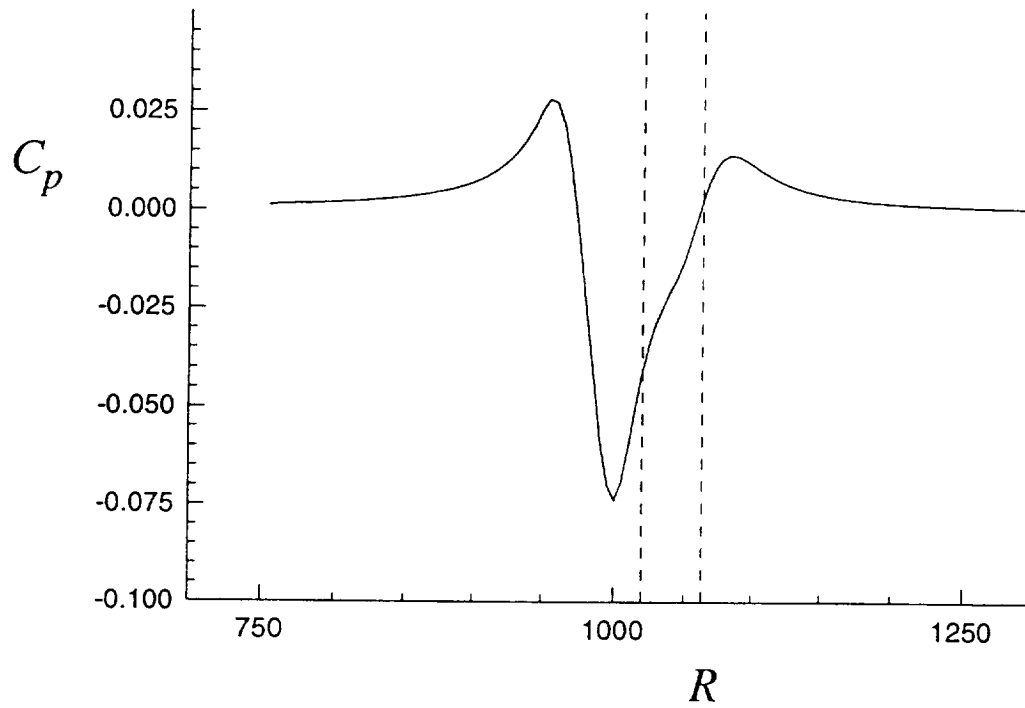


Figure 1. Distribution of pressure coefficient  $C_p$  for incompressible flow over hump with height  $h = 0.004$  at  $Re = 16^6$ . Vertical dashed lines are boundaries of separation bubble, and center of hump is at  $R = 1000$ .

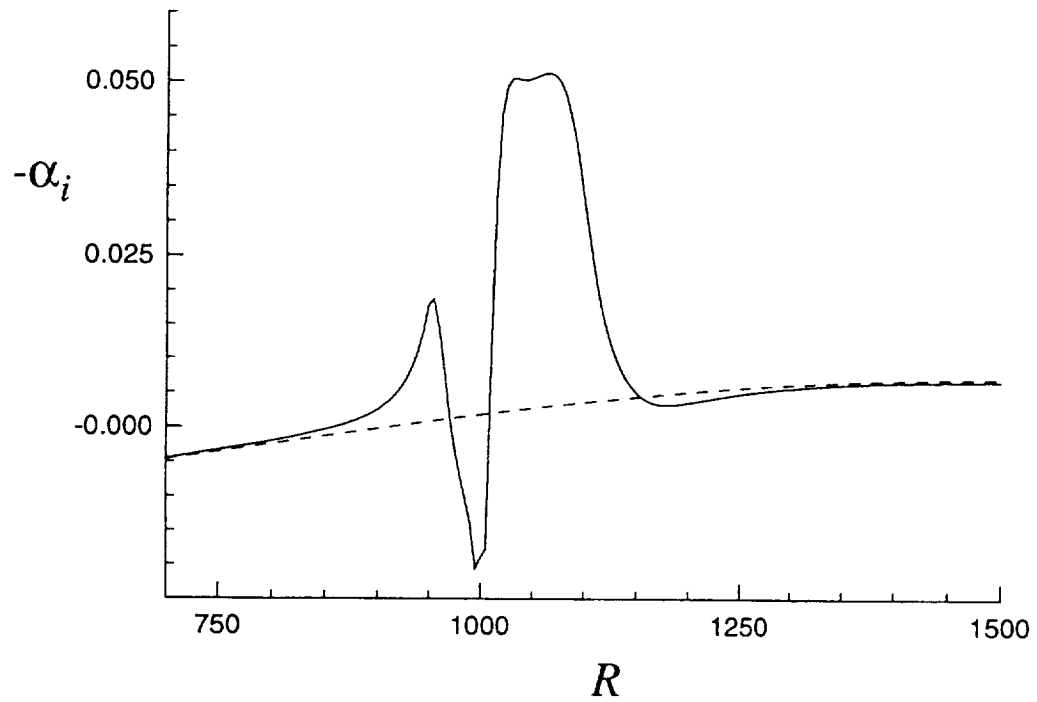


Figure 2. Variation of growth rate with Reynolds number for incompressible flow over (...) a smooth plate and (--) a plate with a hump at  $Re = 10^6$ . Frequency of disturbance is  $F = 25 \times 10^{-6}$ .

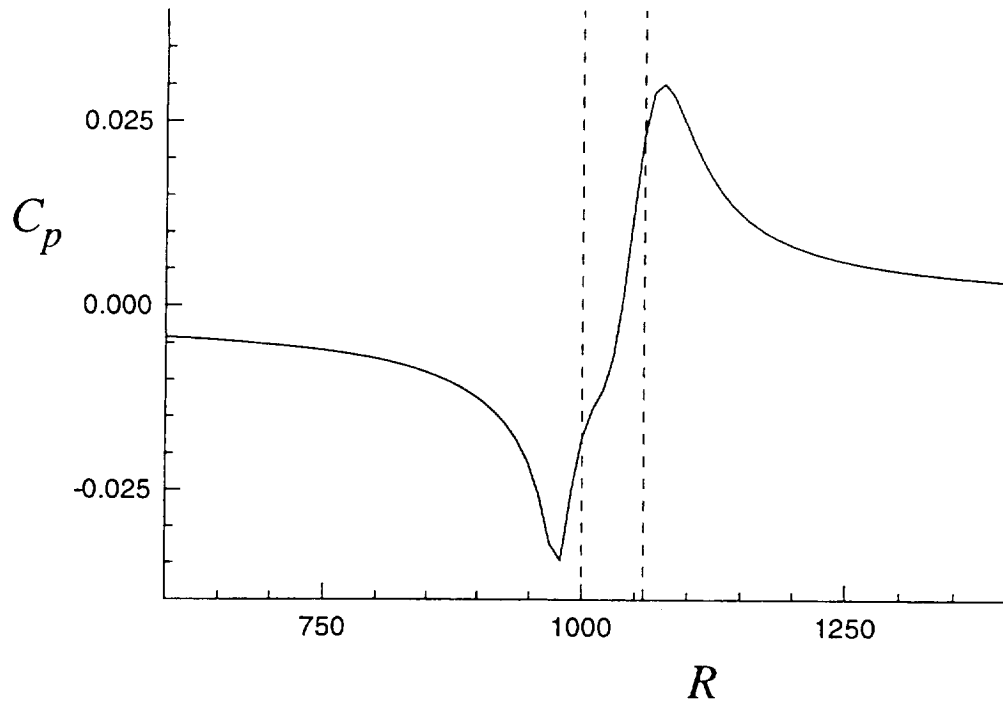


Figure 3. Distribution of pressure coefficient  $C_p$  for incompressible flow over backward-facing step with height  $h = 0.005$  and slope  $s = -5$  at  $Re = 10^6$ . Vertical dashed lines are boundaries of separation bubble. Center of step is at  $R = 1000$ .

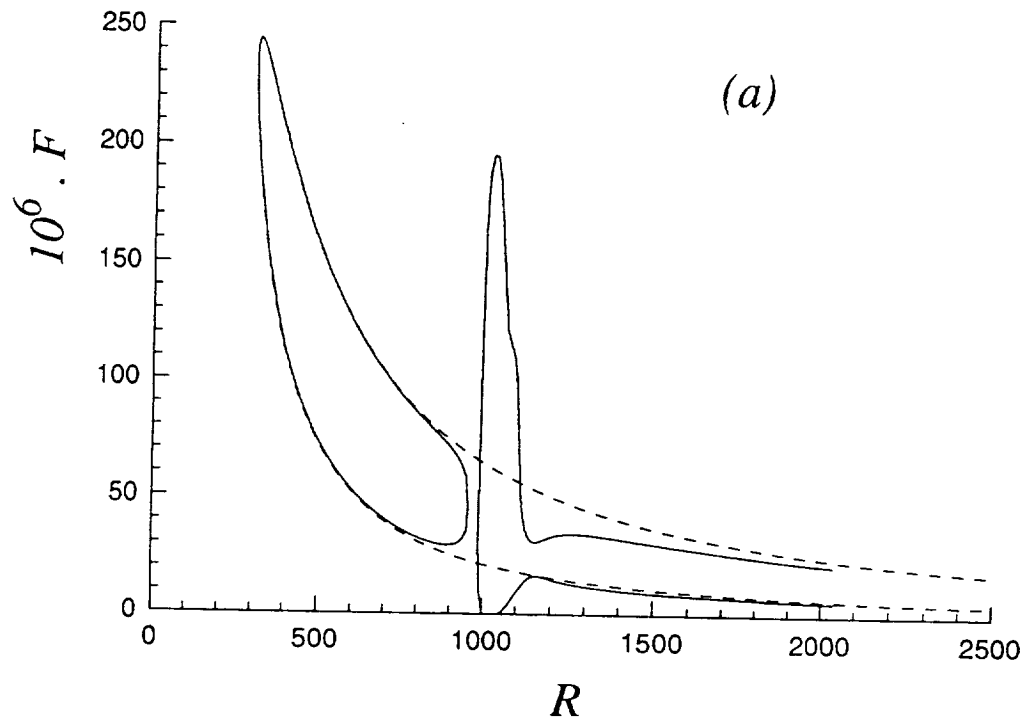


Figure 4. Neutral stability curves for two-dimensional disturbances in incompressible flow with step height  $h = 0.005$ , step slope  $s = -5$ ,  $Re = 10^6$ , and step center at  $R = 1000$ . (a) F-R domain, and (b)  $\alpha_i$ -R domain.



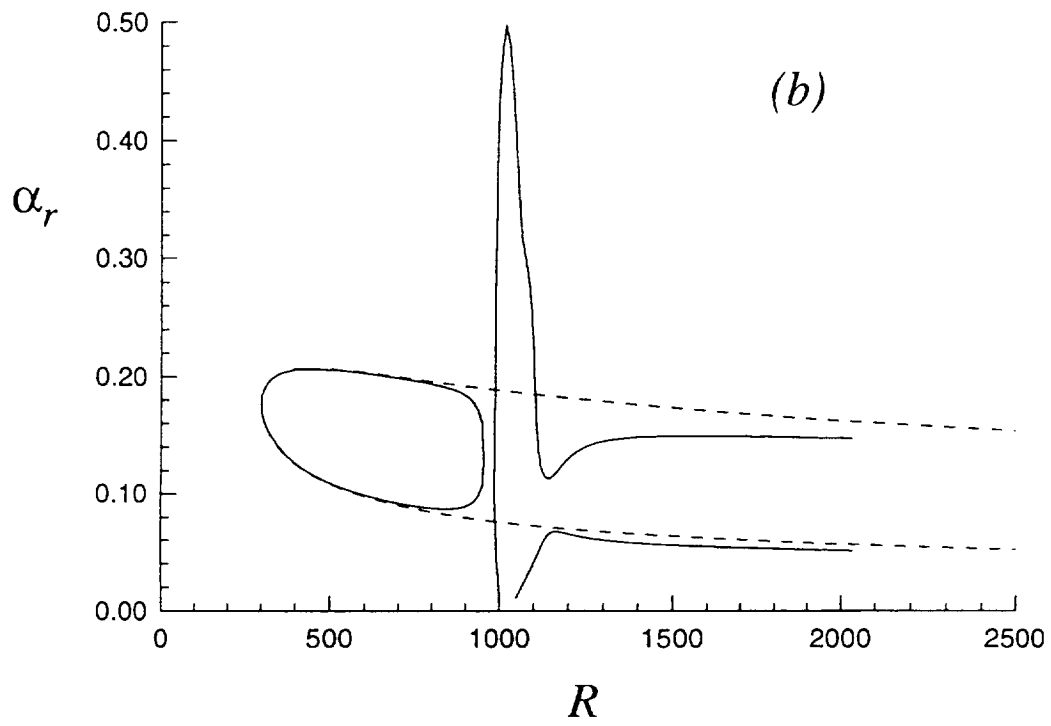


Figure 4. Concluded

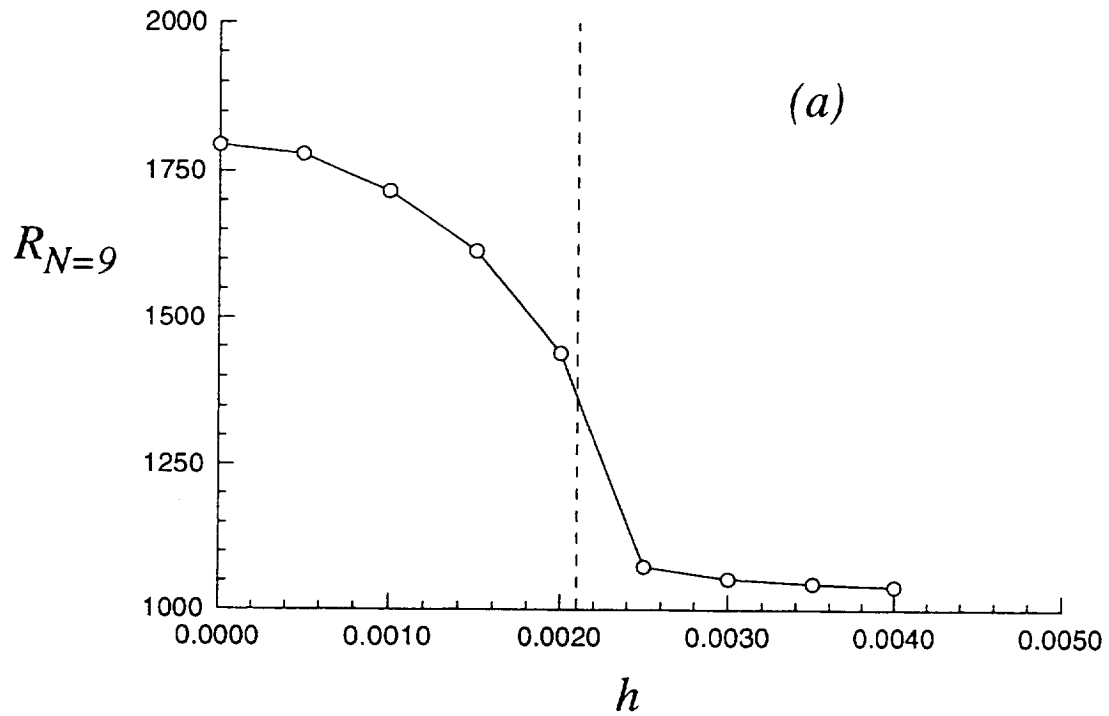


Figure 5. (a) Variation of Reynolds number where  $N$  factor first reaches 9 with hump height for incompressible flow at  $Re = 10^6$ . Vertical dashed line indicates value of hump height that induces incipient separation. Circles indicate locations where calculations were actually made. (b) Corresponding frequencies.

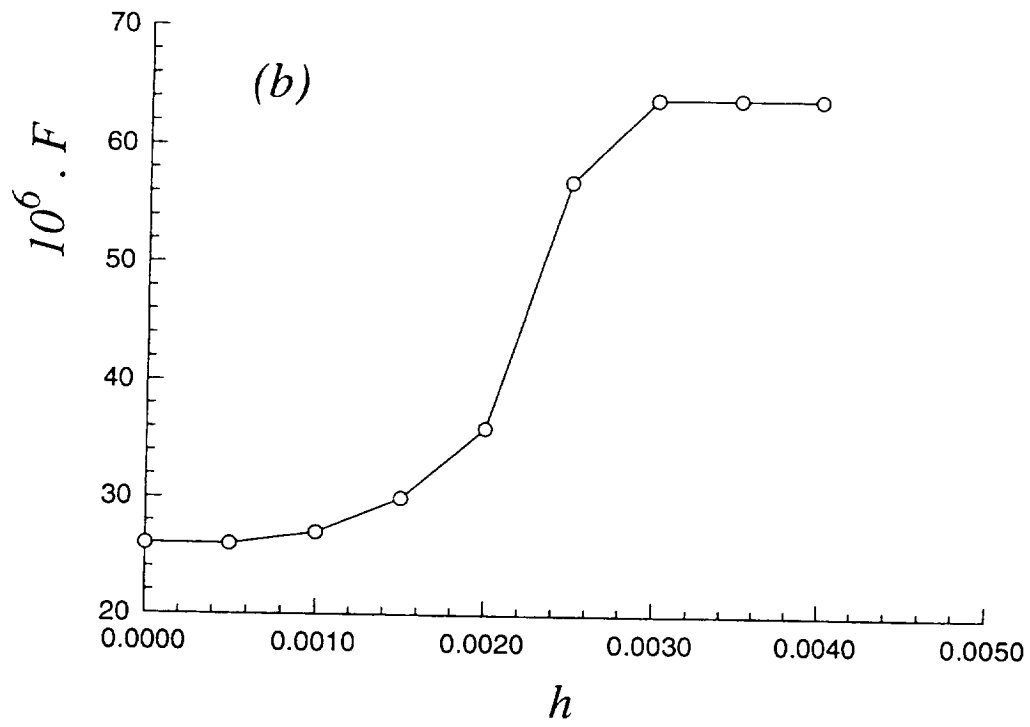


Figure 5. Concluded

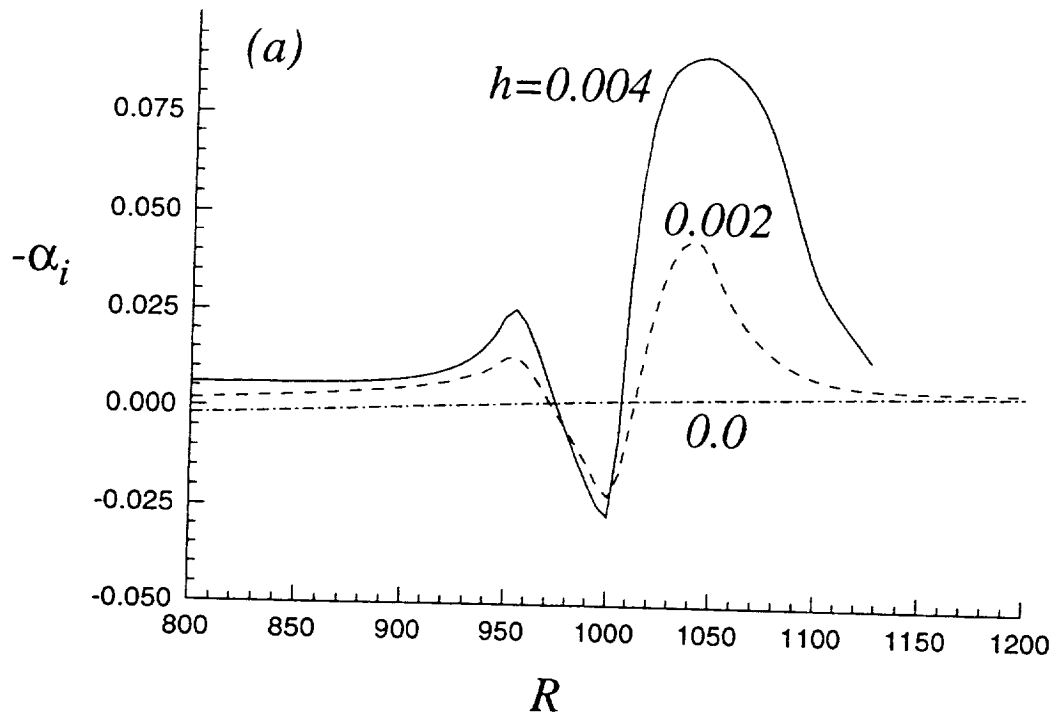


Figure 6. (a) Variation of growth rate with Reynolds number for three cases considered in Figure 5. (b) Corresponding  $N$  factors

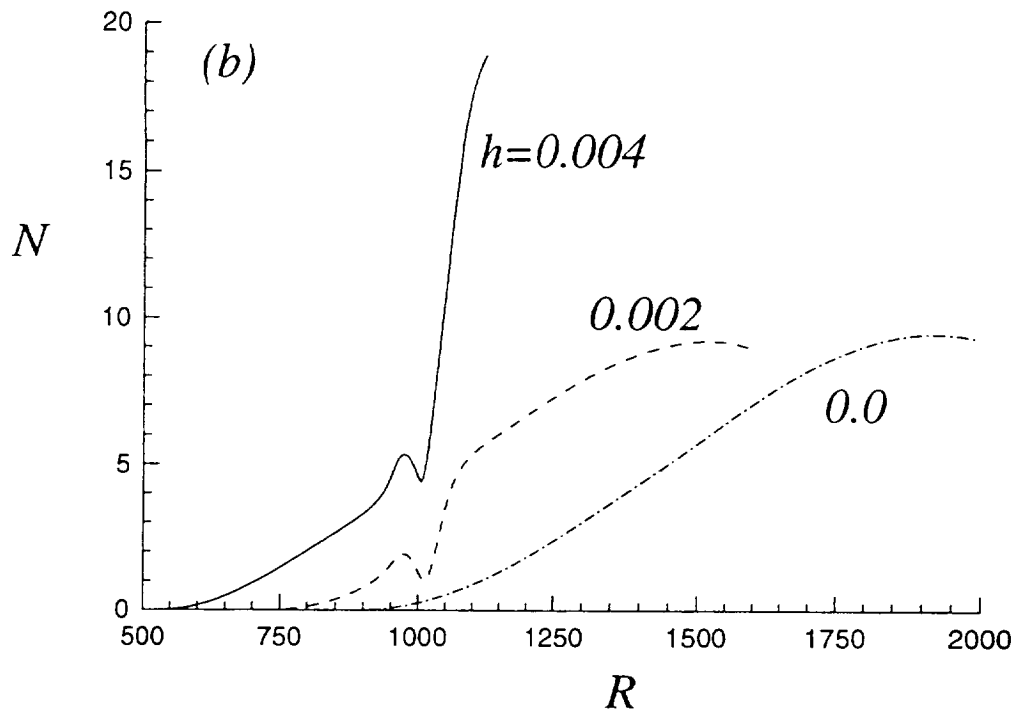


Figure 6. Concluded

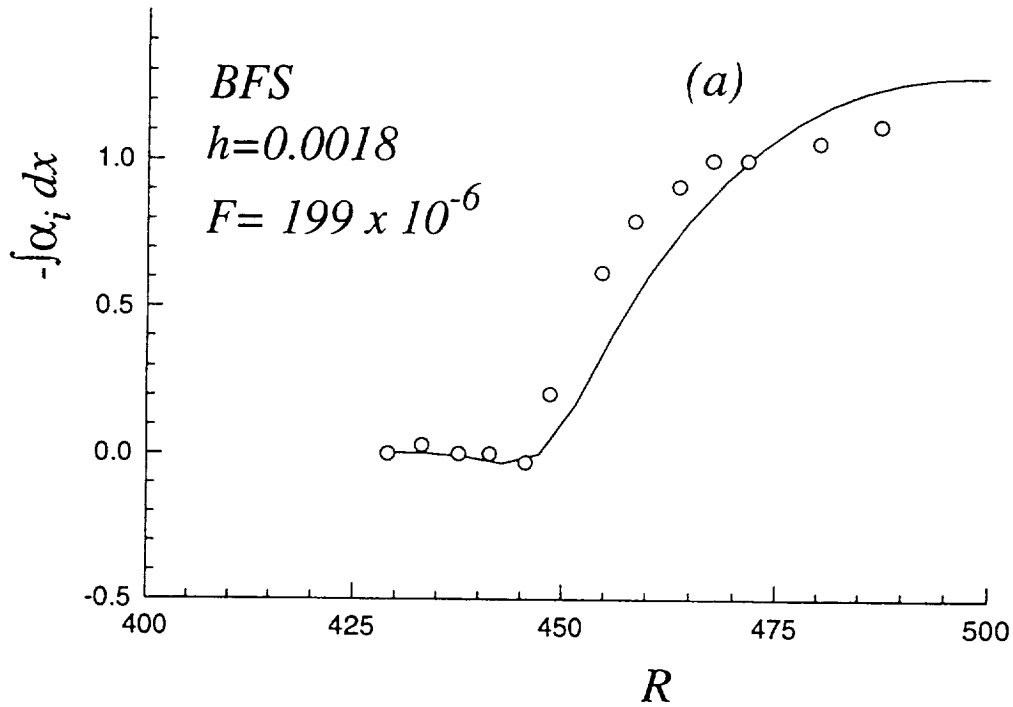


Figure 7. Variation of  $-\int \alpha_i dx$  with Reynolds number for incompressible flow over step at  $Re = 2 \times 10^5$ . (—) Theoretical results and (O) experimental data.

- (a) Backward-facing step, with slope  $s = -10$ , height  $h = 0.0018$ , and  $F = 199 \times 10^{-6}$ ,
- (b) Backward-facing step,  $s = -10$ ,  $h = 0.0018$ ,  $F = 157 \times 10^{-6}$ .
- (c) Backward-facing step,  $s = -10$ ,  $h = 0.0018$ ,  $F = 246 \times 10^{-6}$ .
- (d) Backward-facing step,  $s = -10$ ,  $h = 0.0044$ ,  $F = 157 \times 10^{-6}$ .
- (e) Backward-facing step,  $s = -10$ ,  $h = 0.0044$ ,  $F = 199 \times 10^{-6}$ .
- (f) Backward-facing step,  $s = -10$ ,  $h = 0.0044$ ,  $F = 246 \times 10^{-6}$ .
- (g) Forward-facing step,  $s = 10$ ,  $h = 0.0018$ ,  $F = 157 \times 10^{-6}$ .
- (h) Forward-facing step,  $s = 10$ ,  $h = 0.0018$ ,  $F = 199 \times 10^{-6}$ .
- (i) Forward-facing step,  $s = 10$ ,  $h = 0.0018$ ,  $F = 246 \times 10^{-6}$ .
- (j) Forward-facing step,  $s = 10$ ,  $h = 0.0044$ ,  $F = 157 \times 10^{-6}$ .
- (k) Forward-facing step,  $s = 10$ ,  $h = 0.0044$ ,  $F = 199 \times 10^{-6}$ .
- (l) Forward-facing step,  $s = 10$ ,  $h = 0.0044$ ,  $F = 246 \times 10^{-6}$ .

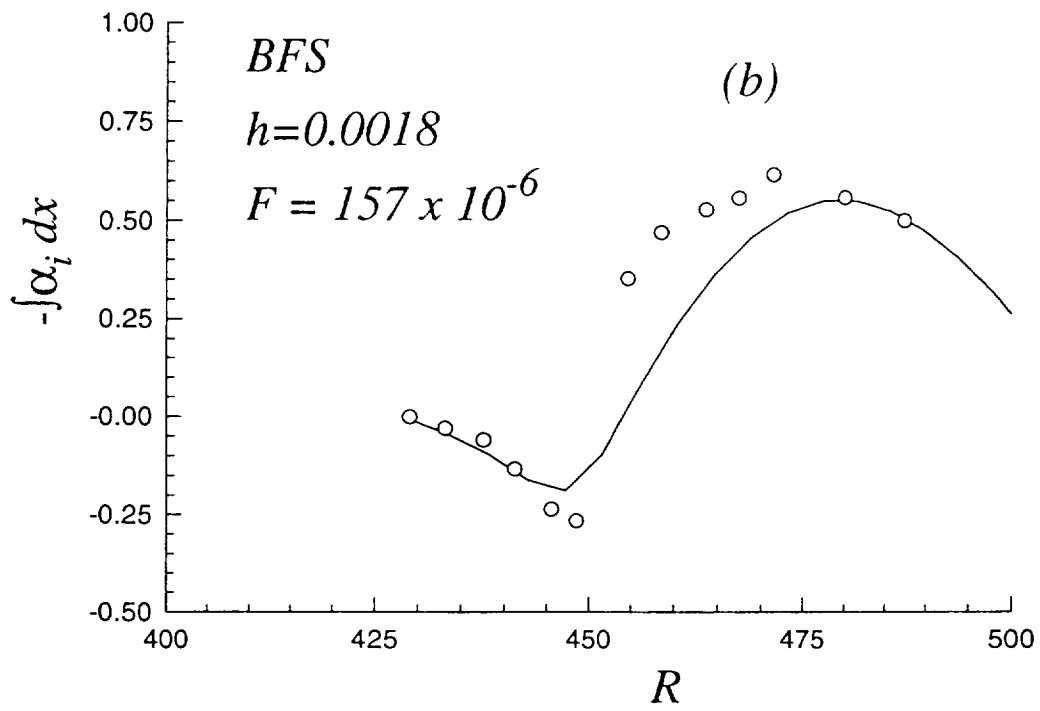


Figure 7. Continued.

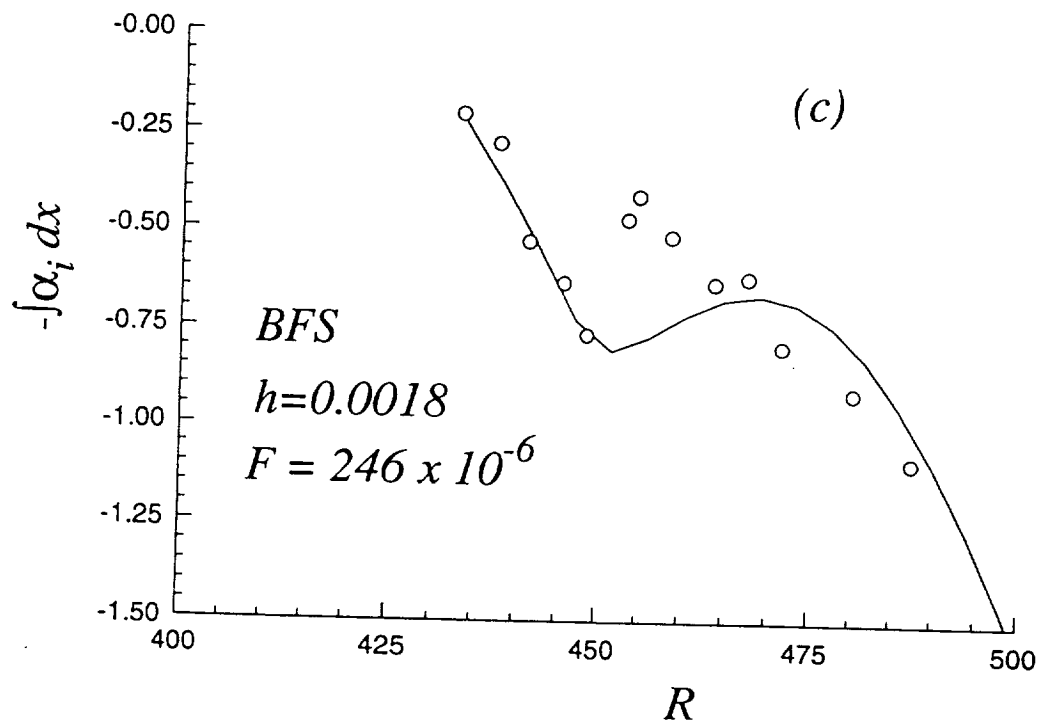


Figure 7. Continued



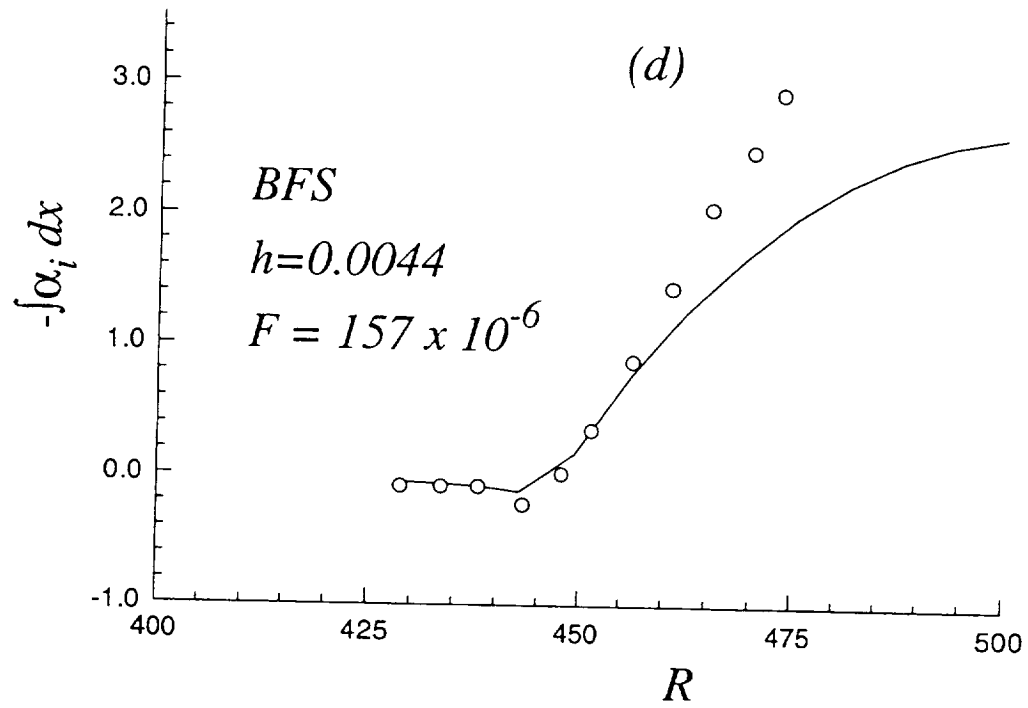


Figure 7. Continued

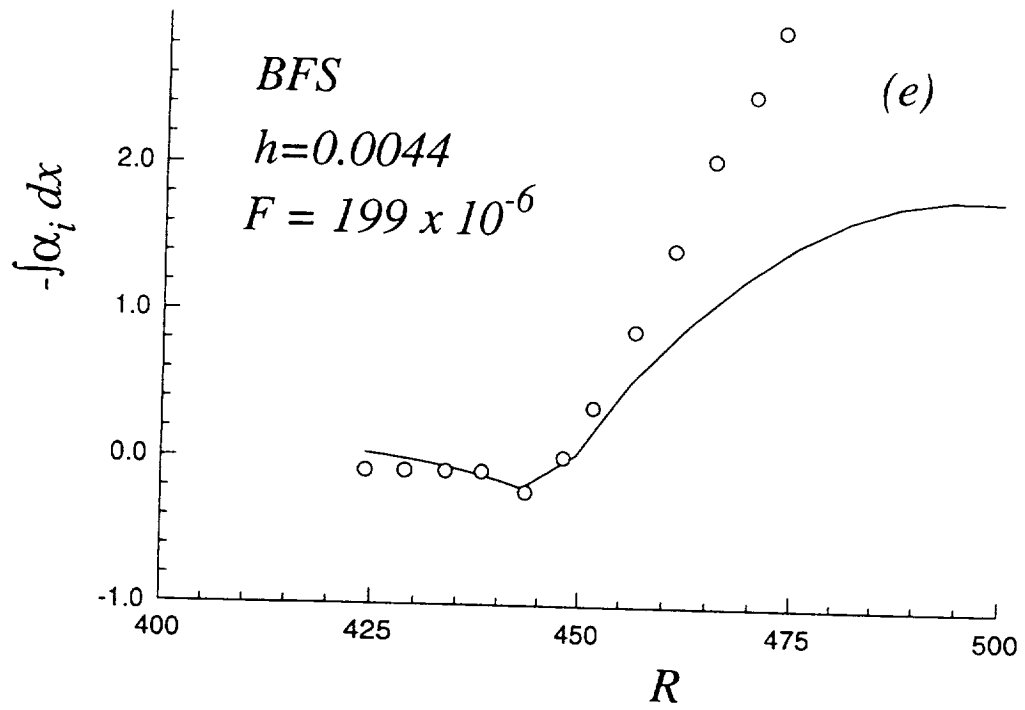


Figure 7. Continued

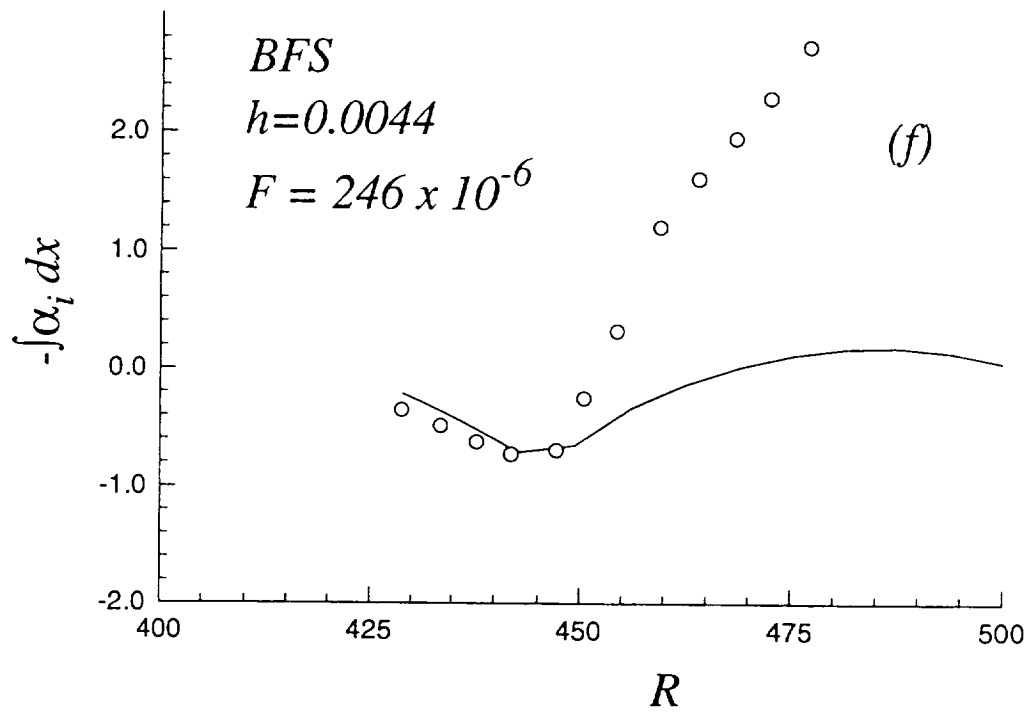


Figure 7. Continued

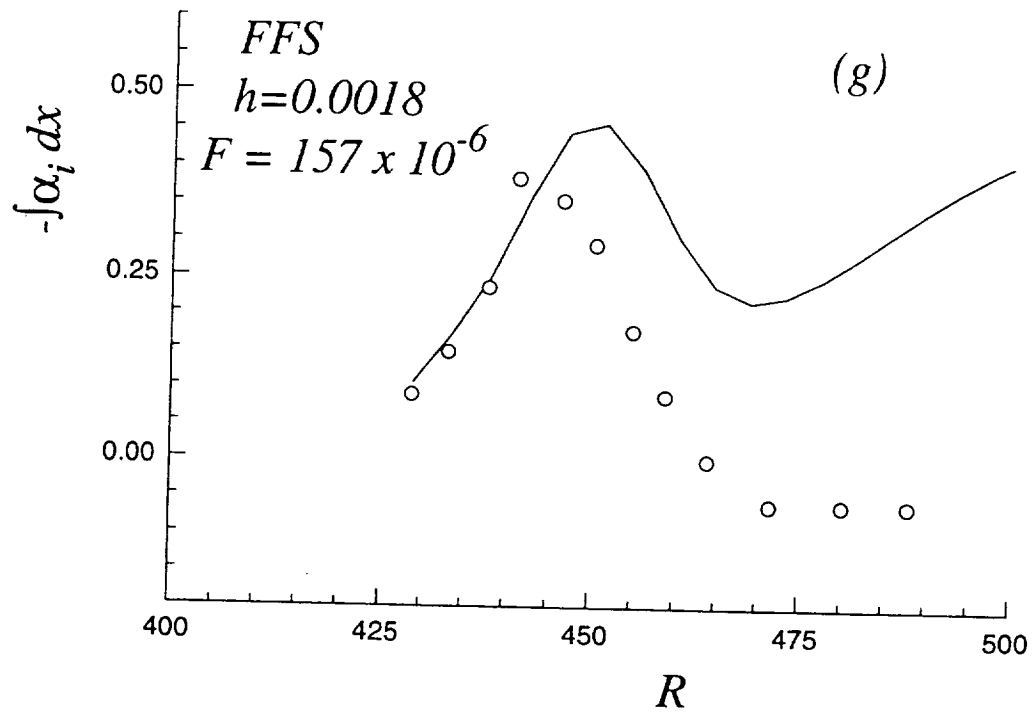


Figure 7. Continued

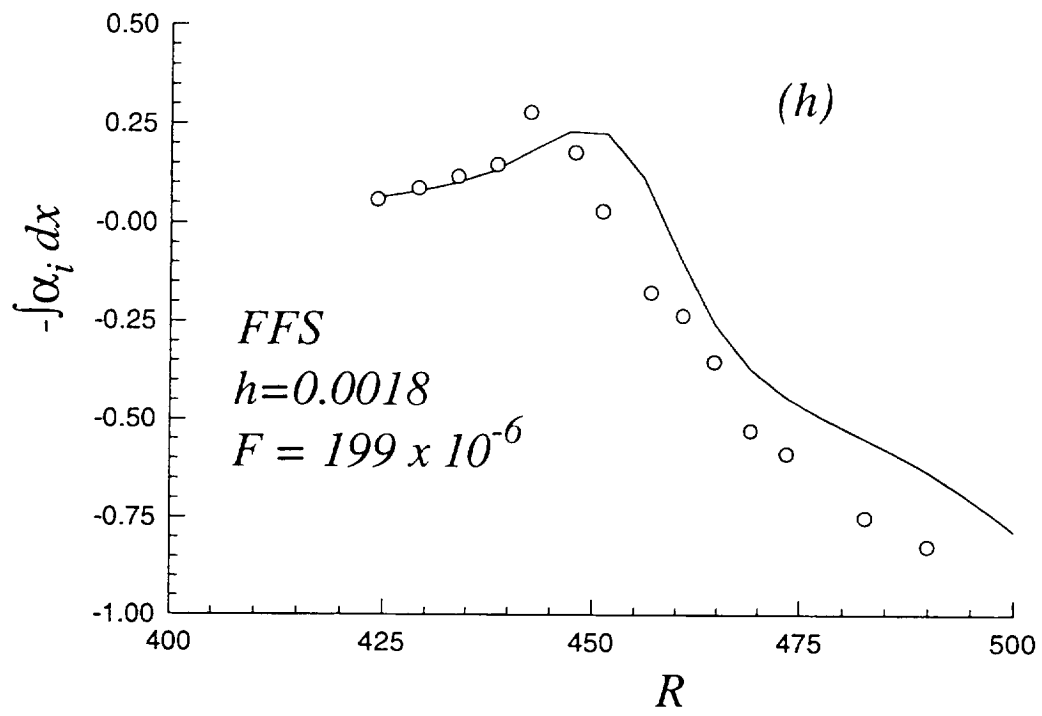


Figure 7. Continued

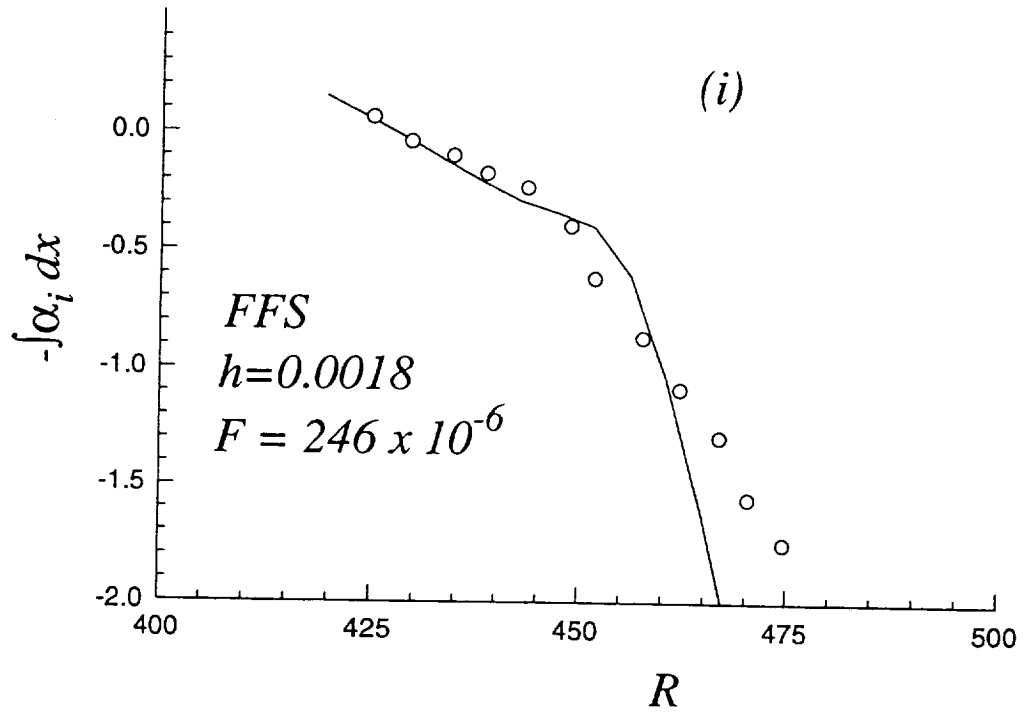


Figure 7. Continued

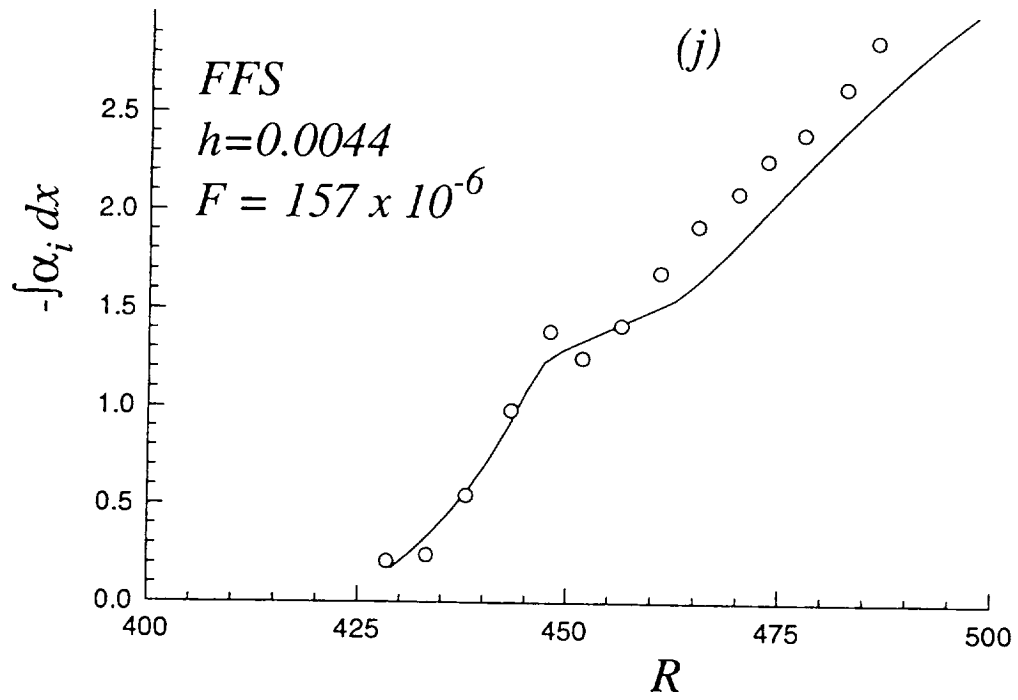


Figure 7. Continued

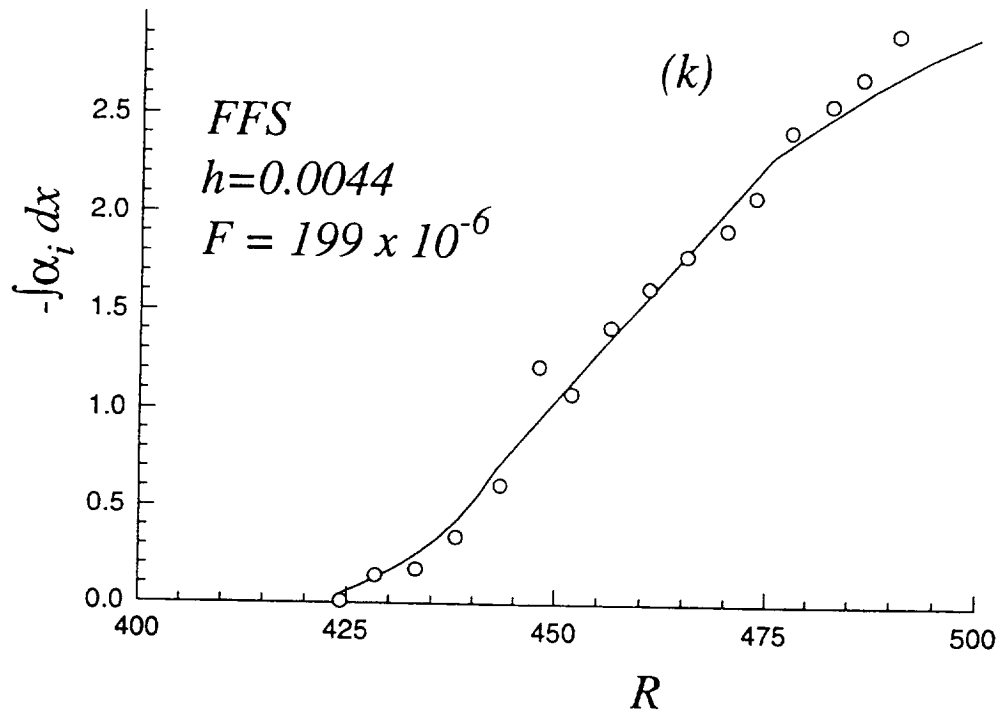


Figure 7. Continued



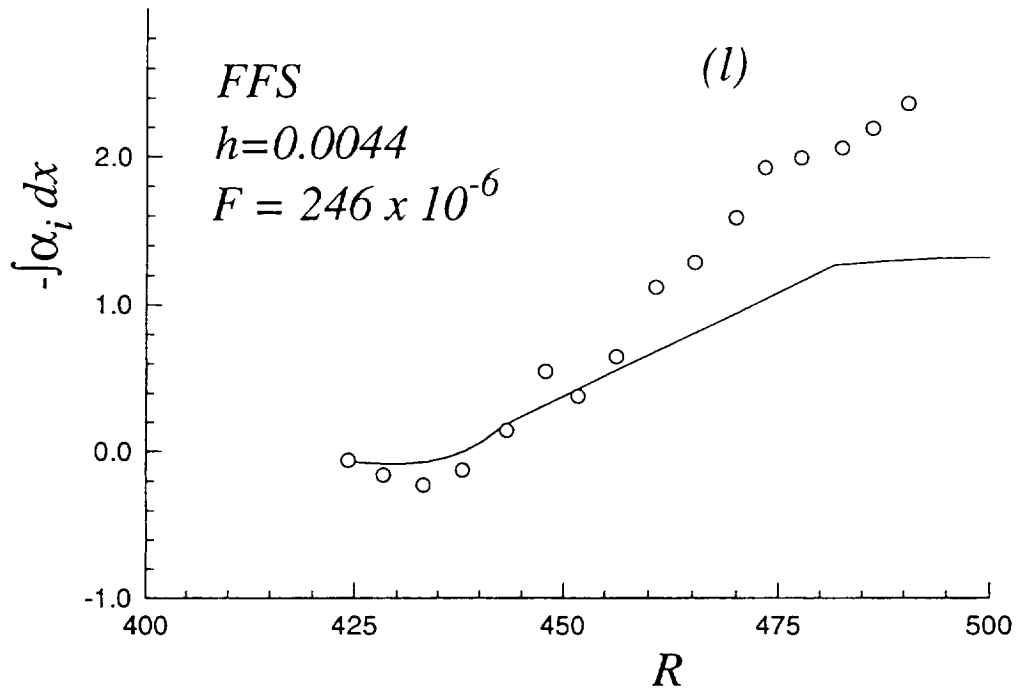


Figure 7. Concluded.

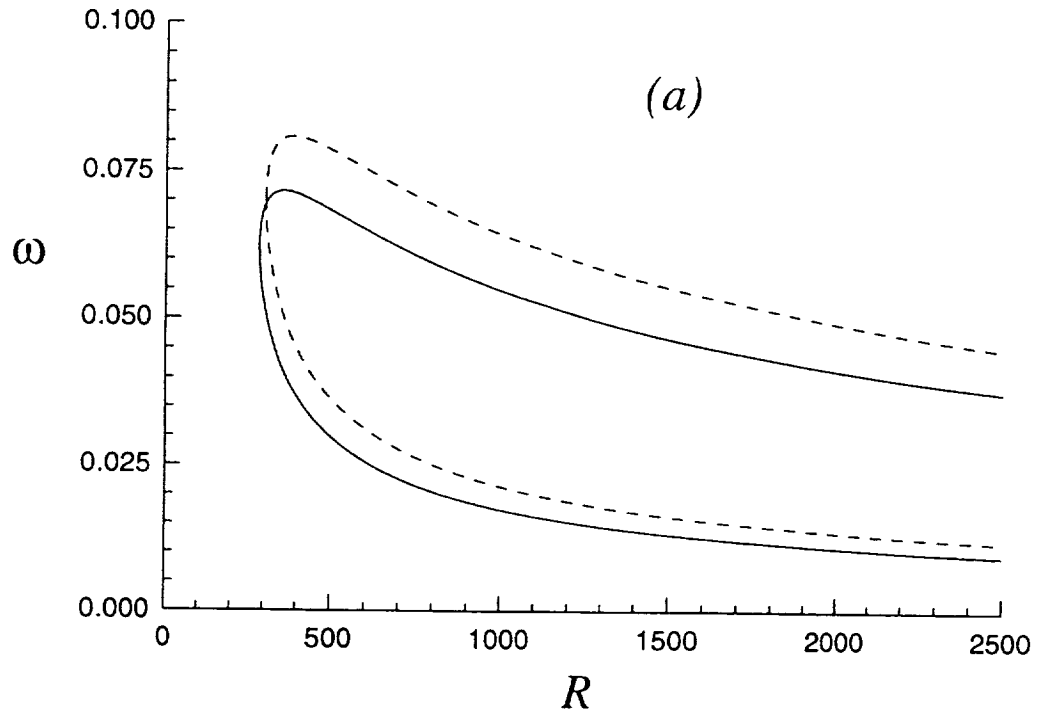


Figure 8. Neutral stability curves of two-dimensional primary disturbances for flow over flat plate. (--)  $M_\infty = 0.8$ , and (...) incompressible flow. (a)  $\omega - R$  domain, and (b)  $\alpha_r - R$  domain.

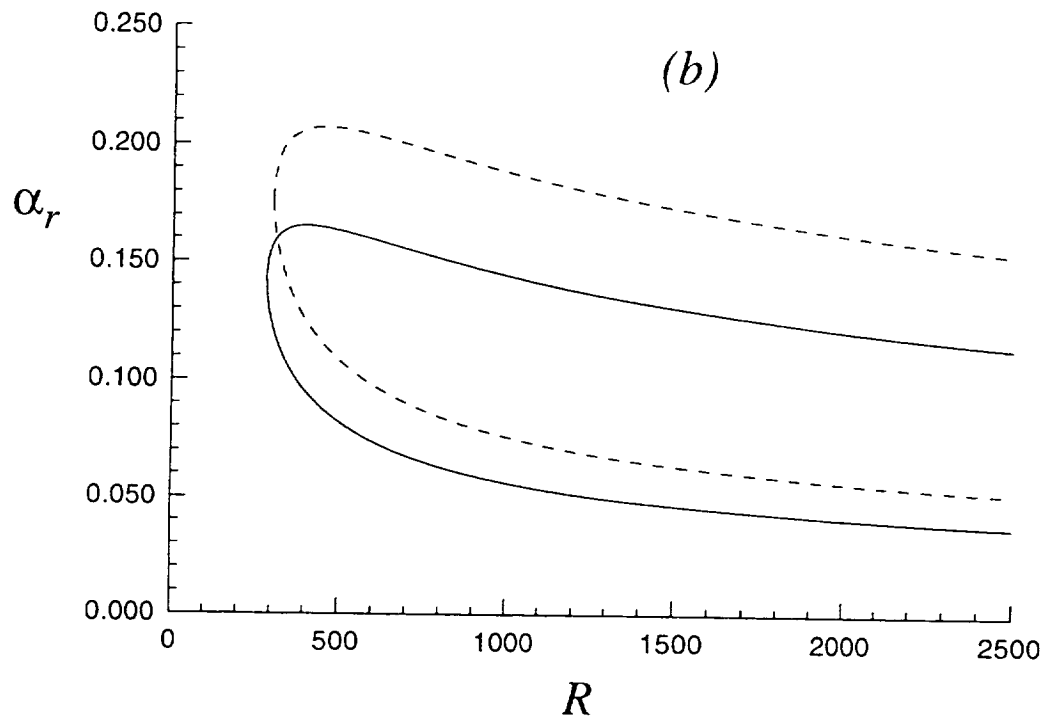


Figure 8. Concluded

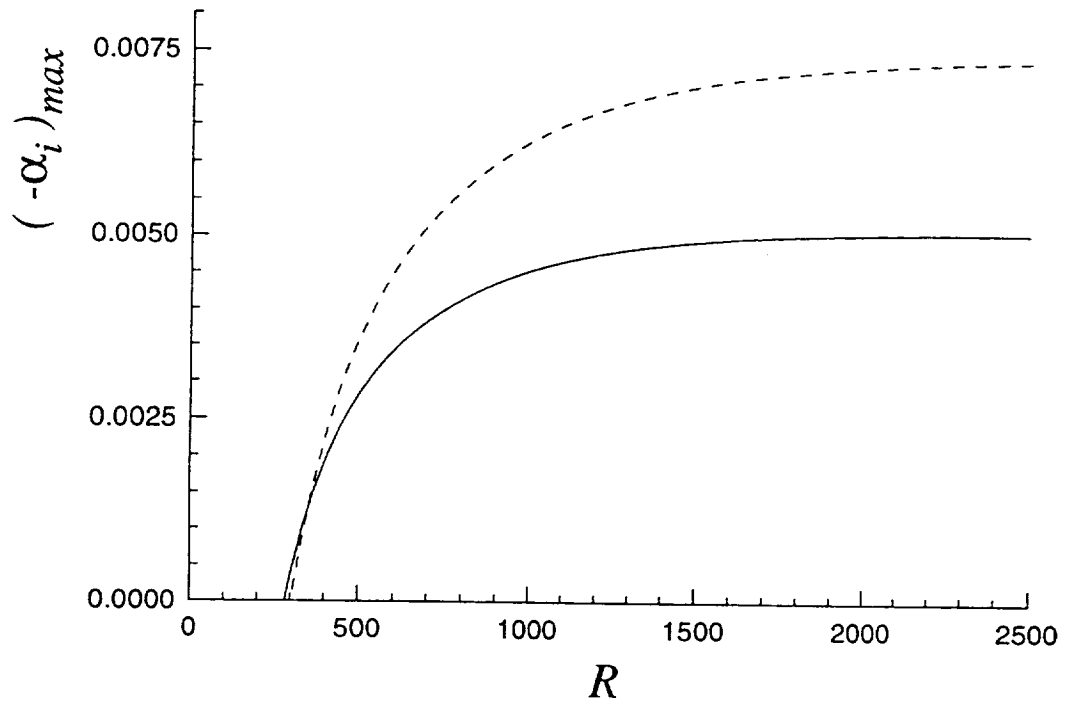


Figure 9. Variation of maximum growth rates (maximized over all frequencies) with  $R$  for two-dimensional primary disturbances in flow over flat plate. (--)  $M_\infty = 0.8$ , and (...) incompressible flow.

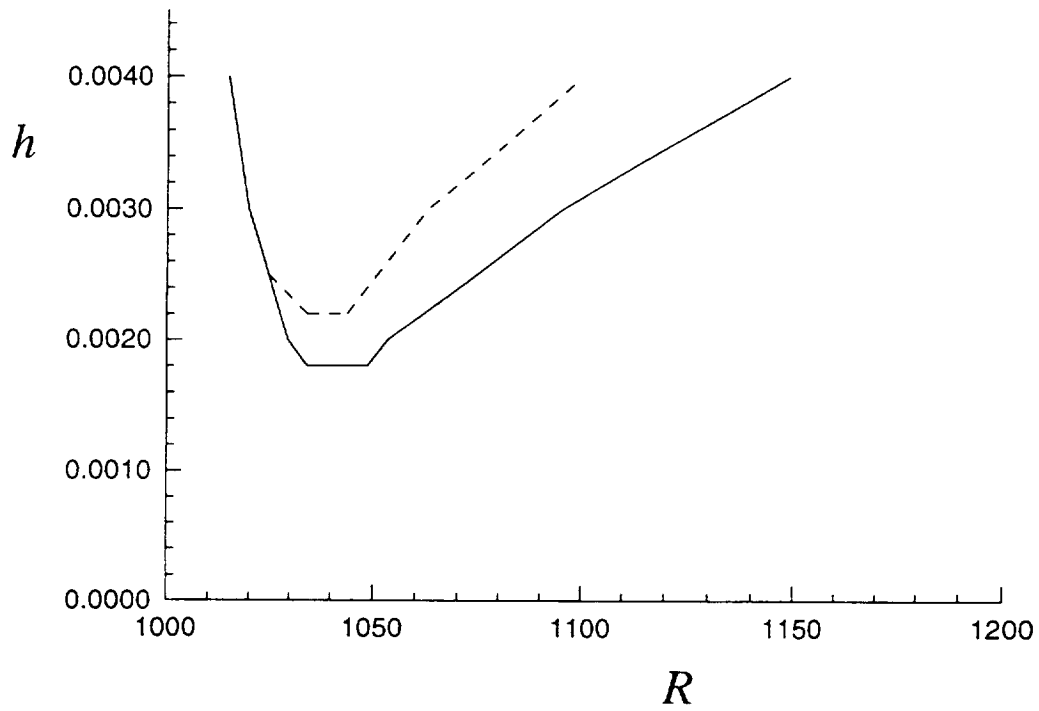


Figure 10. Variation of the streamwise locations of separation and reattachment with hump height when  $Re = 10^6$ . (--)  $M_\infty = 0.8$ , and (...) incompressible flow.

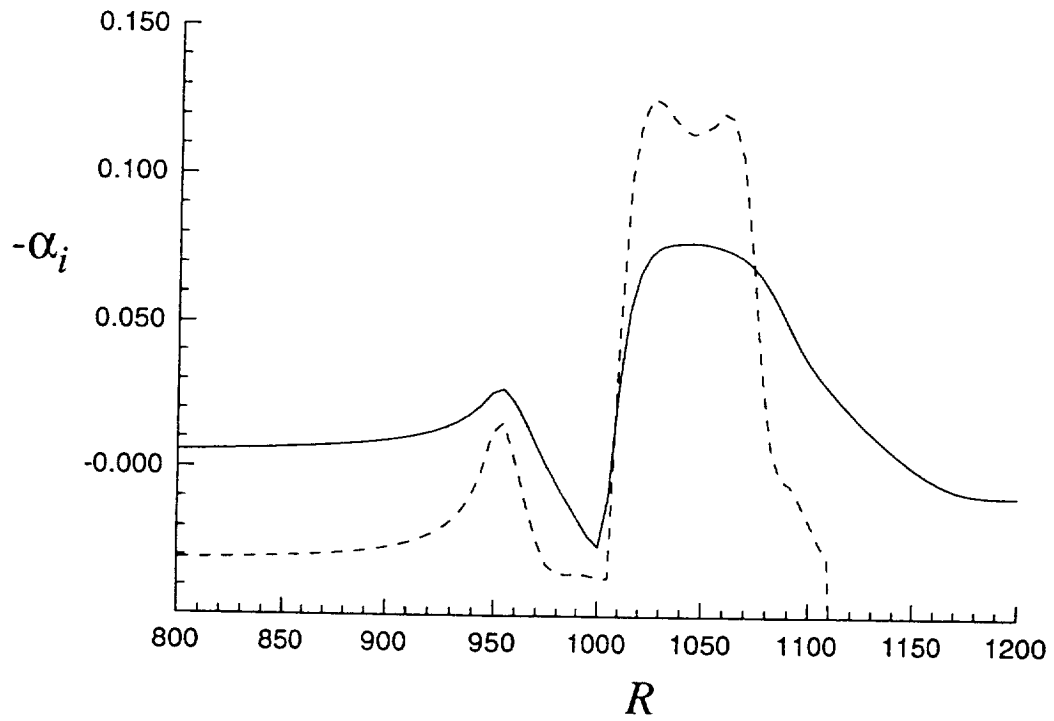


Figure 11. Variation of growth rates of primary waves with  $R$  for incompressible flows over hump where  $F = 50 \times 10^{-6}$ ,  $Re = 10^6$ , and hump height  $h = 0.004$ . (—) Adiabatic conditions, and (...)  $T_w/T_{ad} = 0.5$ .

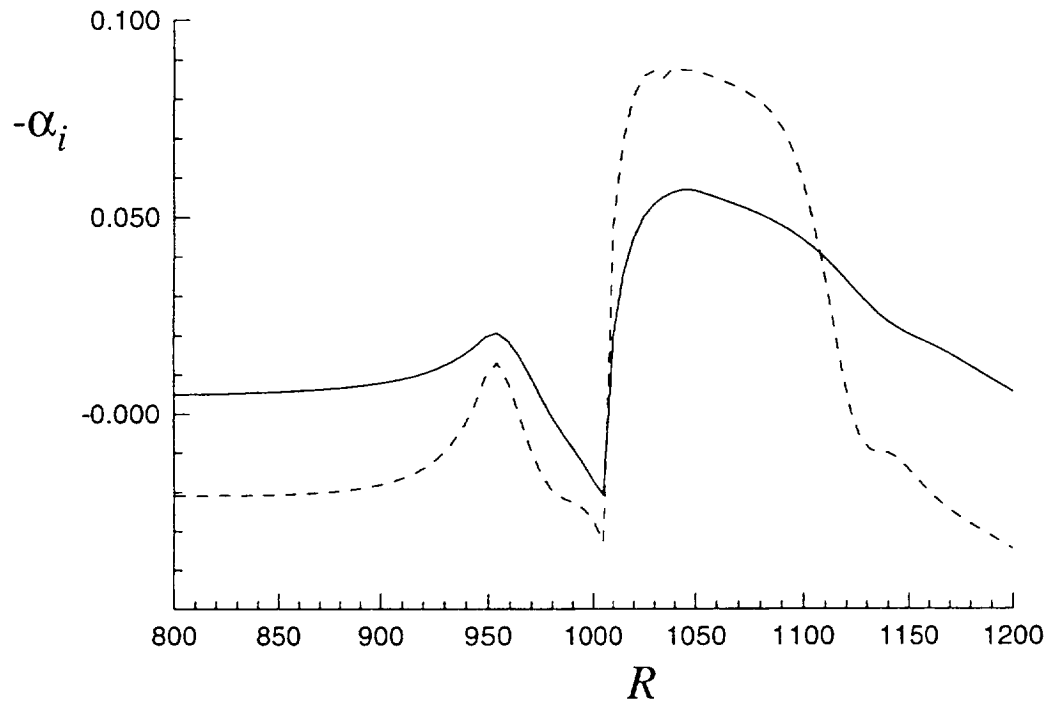


Figure 12. Variation of growth rates of primary waves with  $R$  for subsonic flows over hump where  $M_\infty = 0.8$ ,  $F = 50 \times 10^{-6}$ ,  $Re = 10^6$ , and hump height  $h = 0.004$ . (--) Adiabatic conditions, and (...)  $T_w/T_{ad} = 0.5$ .

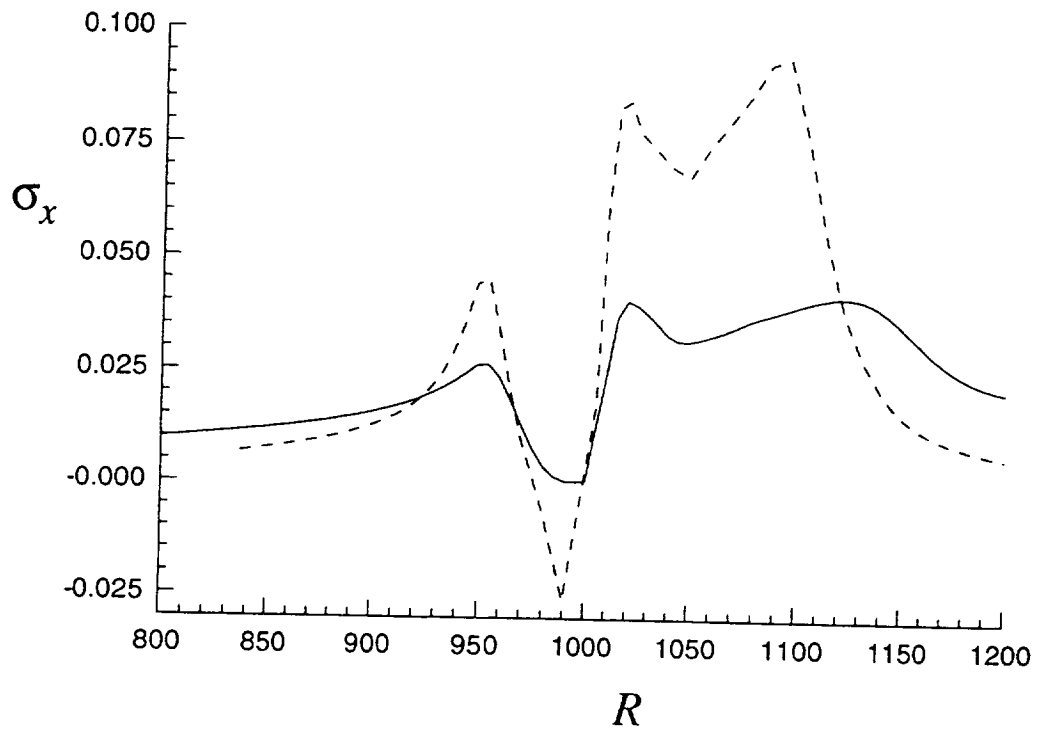


Figure 13. Variation of growth rates of subharmonic waves with  $R$  for subsonic flows over hump where  $M_\infty = 0.8$ ,  $F_{2-D} = 50 \times 10^{-6}$ ,  $B = 0.2$ ,  $Re = 10^6$ , rms amplitude of primary wave is fixed at all values of  $R$  and is equal to 0.01, and hump height  $h = 0.004$ . (--) Adiabatic conditions, and (...)  $T_w/T_{ad} = 0.5$ .



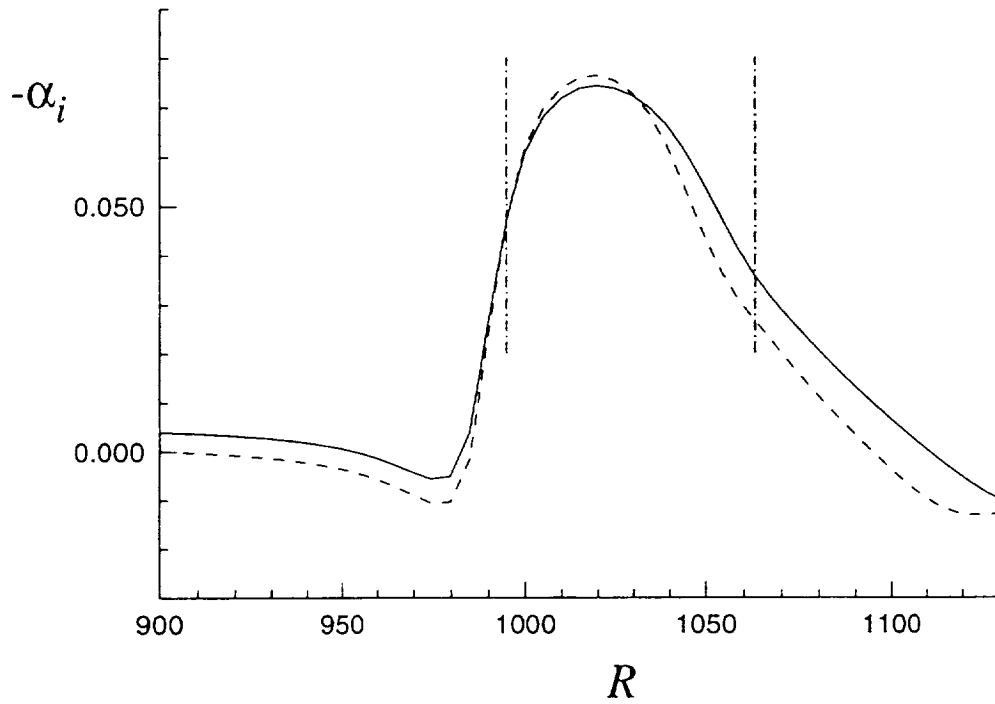


Figure 14. Variation of growth rates of primary waves with  $R$  for incompressible flows over backward-facing step at  $F = 50 \times 10^{-6}$ ,  $Re = 10^6$ , step height  $h = 0.005$ , step slopes =  $-5$ , and center of step is at  $R = 1000$ . (—) No suction, and (---) uniform suction with  $v_w = -1.0 \times 10^{-4}$ .

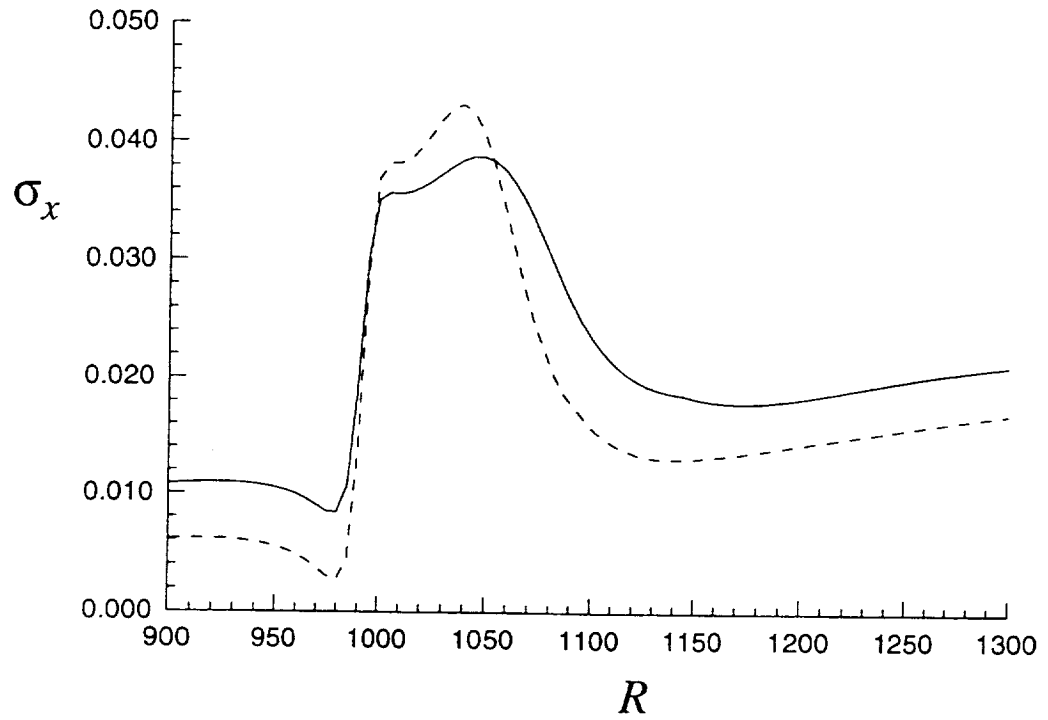


Figure 15. Variation of growth rates of subharmonic waves with  $R$  for subsonic flows over backward-facing step where  $M_\infty = 0.8$ ,  $F_{2-D} = 50 \times 10^{-6}$ ,  $B = 0.2$ ,  $Re = 10^6$ , rms amplitude of primary wave is fixed at all values of  $R$  and is equal to 0.01, the step height  $h = 0.004$ , the step slopes =  $-5$ , and center of step is at  $R = 1000$ . (--) No suction, and (...) uniform suction with  $v_w = -2.0 \times 10^{-4}$ .

REPORT DOCUMENTATION PAGE			Form Approved OMB No. 0704-0188	
Public reporting burden for this collection of information is estimated to average 1 hour per response, including the time for reviewing instructions, searching existing data sources, gathering and maintaining the data needed, and completing and reviewing the collection of information. Send comments regarding this burden estimate or any other aspect of this collection of information, including suggestions for reducing this burden, to Washington Headquarters Services, Directorate for Information Operations and Reports, 1215 Jefferson Davis Highway, Suite 1204, Arlington, VA 22202-4302, and to the Office of Management and Budget, Paperwork Reduction Project (0704-0188), Washington, DC 20503.				
1. AGENCY USE ONLY (Leave blank)		2. REPORT DATE December 1994		3. REPORT TYPE AND DATES COVERED Contractor Report
4. TITLE AND SUBTITLE Stability of Separating Subsonic Boundary Layers			5. FUNDING NUMBERS C NAS1-19299 C NAS1-19610  WU 538-05-15-01	
6. AUTHOR(S) Jamal A. Masad Ali H. Nayfeh				
7. PERFORMING ORGANIZATION NAME(S) AND ADDRESS(ES) High Technology Corporation 28 Research Drive Hampton, VA 23666 Virginia Polytechnic Institute and State University ESM Department Blacksburg, VA 24061			8. PERFORMING ORGANIZATION REPORT NUMBER	
9. SPONSORING / MONITORING AGENCY NAME(S) AND ADDRESS(ES) National Aeronautics and Space Administration Langley Research Center Hampton, VA 23681-0001			10. SPONSORING / MONITORING AGENCY REPORT NUMBER NASA CR-4638	
11. SUPPLEMENTARY NOTES Langley Technical Monitor: Ajay Kumar				
12a. DISTRIBUTION / AVAILABILITY STATEMENT Unclassified/Unlimited Subject Category 34			12b. DISTRIBUTION CODE	
13. ABSTRACT (Maximum 200 words) The primary and subharmonic instabilities of separating compressible subsonic two-dimensional boundary layers in the presence of a two-dimensional roughness element on a flat plate are investigated. The roughness elements considered are humps and forward- and backward-facing steps. The use of cooling and suction to control these instabilities is studied. The similarities and differences between the instability characteristics of separating boundary layers and those of the boundary layer over a flat plate with a zero pressure gradient are pointed out and discussed. The theoretical results agree qualitatively and quantitatively with the experimental data of Dovgal and Kozlov. Cooling and suction decrease the growth rates of primary and subharmonic waves in the attached-flow regions but increase them in the separated-flow regions.				
14. SUBJECT TERMS Stability, Separation, Roughness			15. NUMBER OF PAGES 49	
			16. PRICE CODE A03	
17. SECURITY CLASSIFICATION OF REPORT Unclassified	18. SECURITY CLASSIFICATION OF THIS PAGE Unclassified	19. SECURITY CLASSIFICATION OF ABSTRACT Unclassified	20. LIMITATION OF ABSTRACT	





National Aeronautics and  
Space Administration  
Langley Research Center  
Mail Code 180  
Hampton, VA 23681-00001

**Official Business**  
Penalty for Private Use, \$300

**BULK RATE**  
**POSTAGE & FEES PAID**  
NASA  
Permit No. G-27